Vacancy clusters in ultra fine grained metals prepared by severe plastic deformation

J. Čížek, O. Melikhova, Z. Barnovská, I. Procházka

Faculty of Mathematics and Physics, Charles University Prague, Czech Republic

R. K. Islamgaliev

Institute of Physics of Advanced Materials, Ufa State Aviation Technical University, Ufa, Russia

S.V. Dobatkin

A. A. Baikov Institute of Metallurgy and Materials Science, Russian Academy of Sciences, Moscow, Russia

Outline

- vacancies introduced by severe plastic deformation
- *ab-initio* theoretical modeling of vacancy clusters
- size distribution of vacancy clusters
- mapping of spatial distribution of vacancy clusters

Ultra fine grained (UFG) materials

polycrystalline material

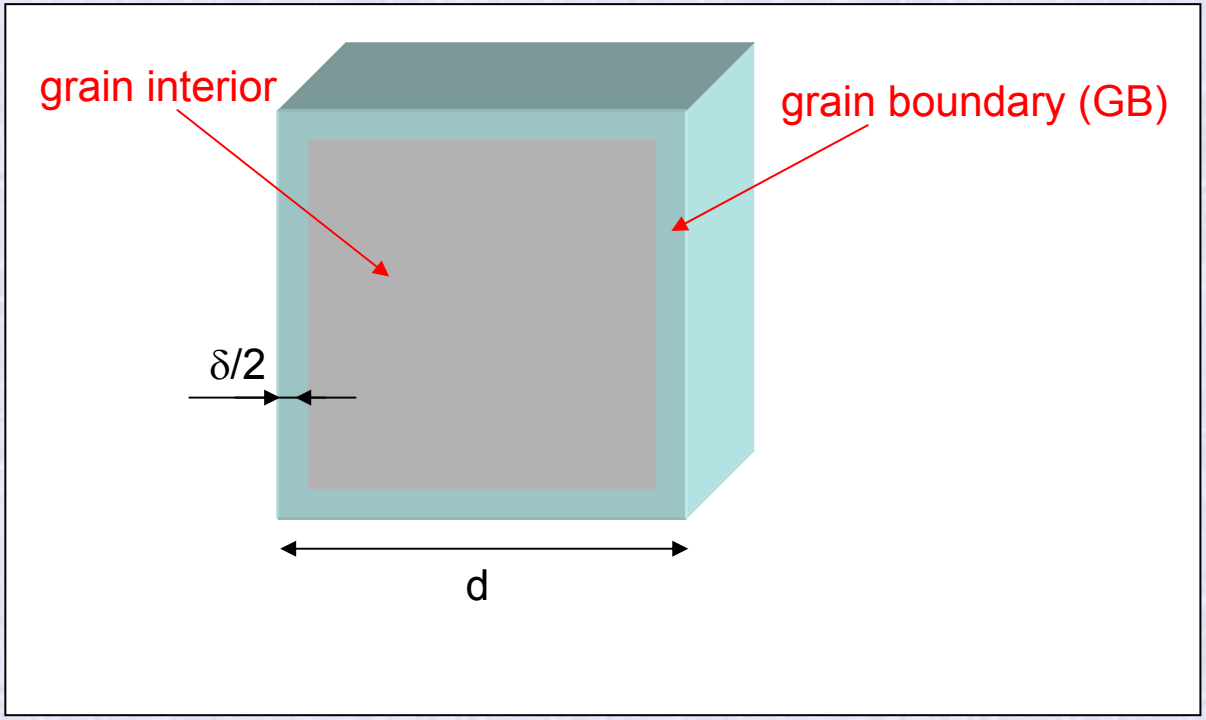

volume fraction of GB's

$$f_{GB} = 1 - \left(\frac{d - \delta}{d} \right)^3$$

Ultra fine grained (UFG) materials

polycrystalline material

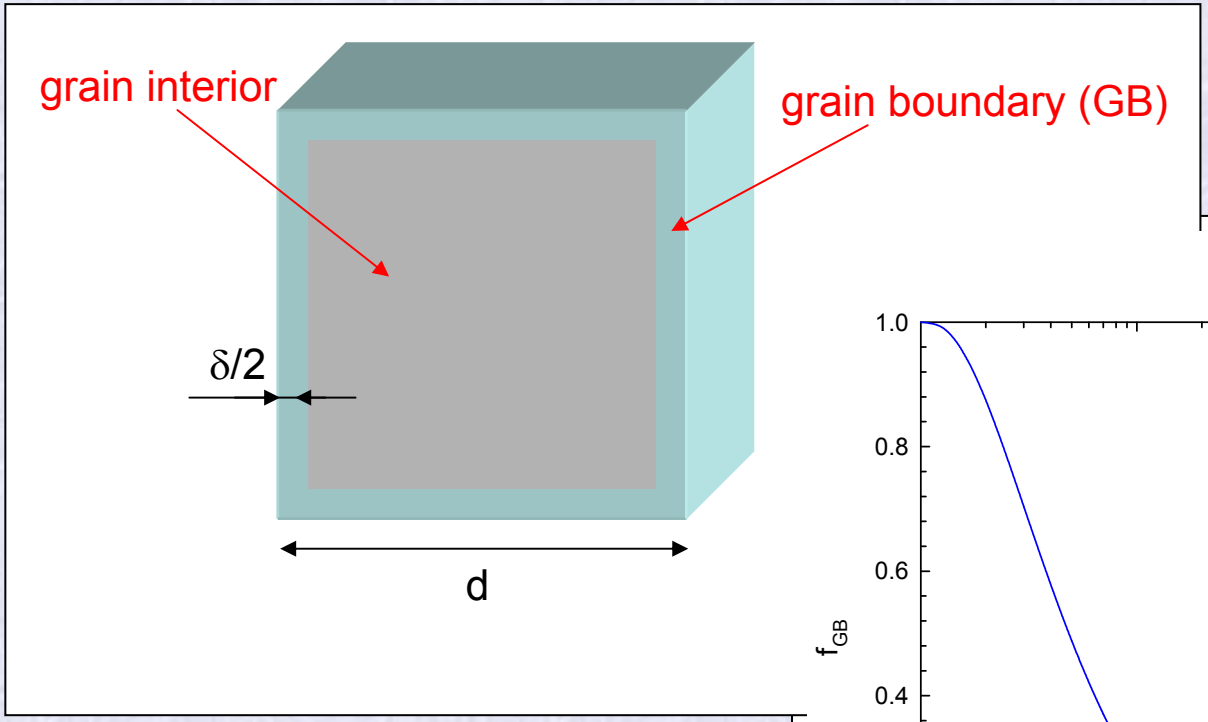

crystallographic width of GB's: $\delta \approx 1$ nm

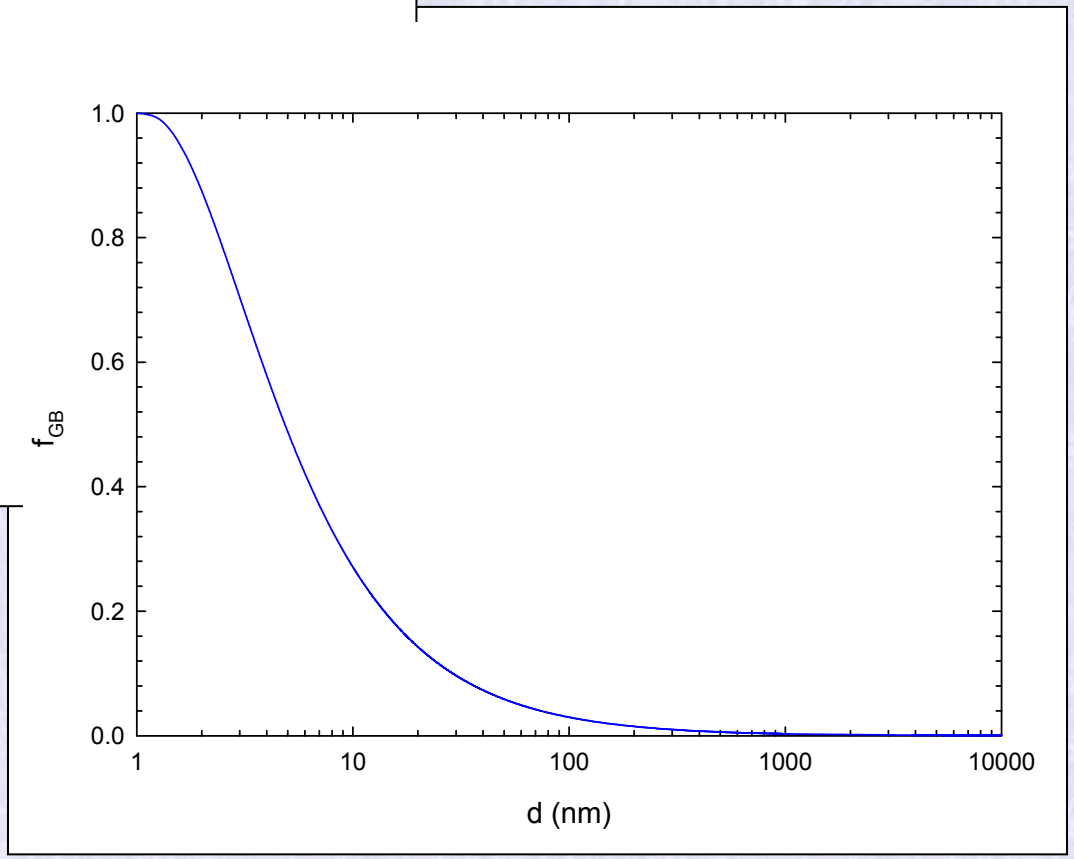

volume fraction of GB's

$$f_{GB} = 1 - \left(\frac{d - \delta}{d} \right)^3$$

Ultra fine grained (UFG) materials

polycrystalline material

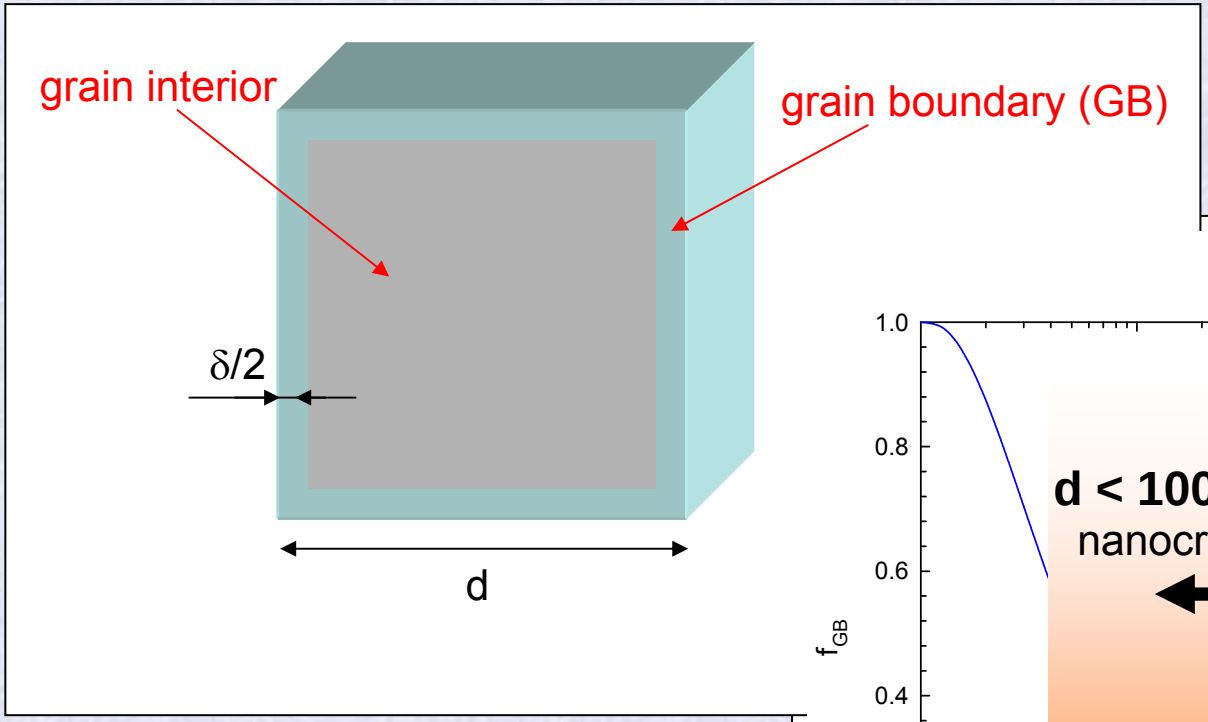

crystallographic width of GB's: $\delta \approx 1$ nm

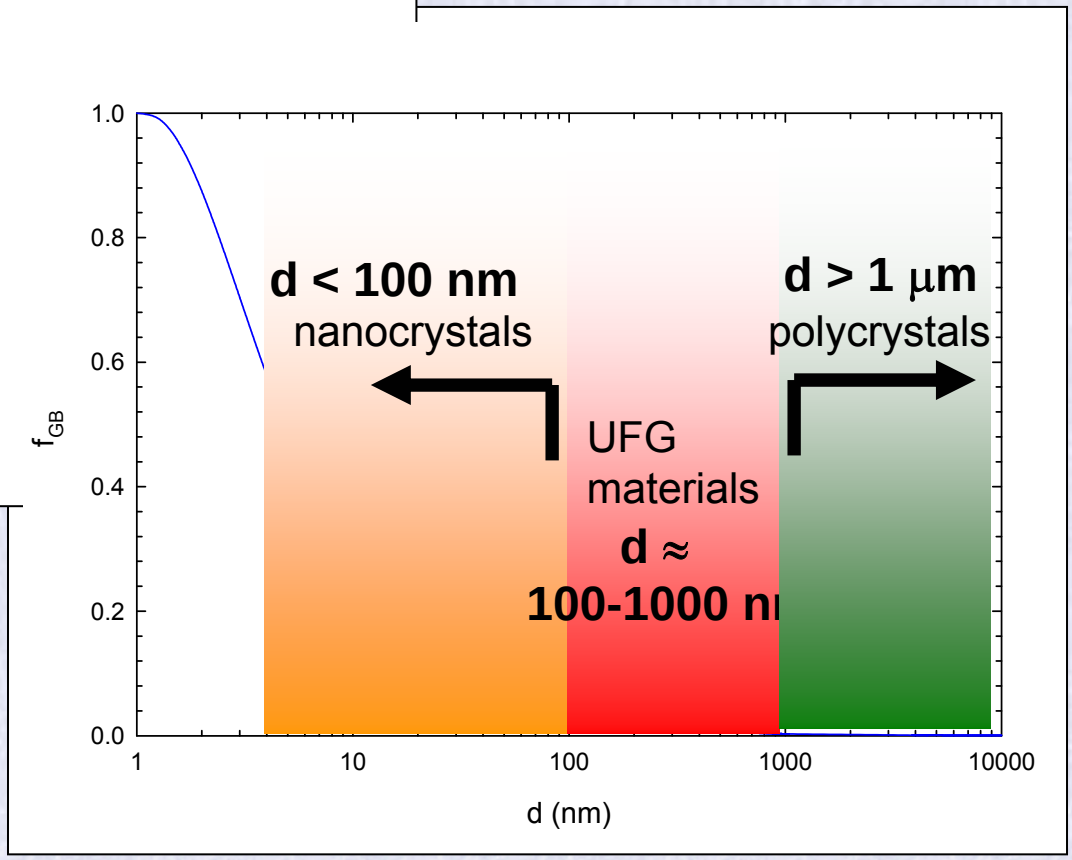

volume fraction of GB's

$$f_{GB} = 1 - \left(\frac{d - \delta}{d} \right)^3$$

Introduction

Severe plastic deformation

- very strong grain size reduction → down to nanoscale (~ 100 nm)

- P.W. Bridgman, 1930 , Harvard University
  Large hydrostatic presure (10 GPa) + shear deformation
  Nobel prize in Physics 1946

- R.Z. Valiev, 1980 , Ufa State Aviation Technical University
  High pressure torsion (HPT)
  Equal channel angular pressing (ECAP)

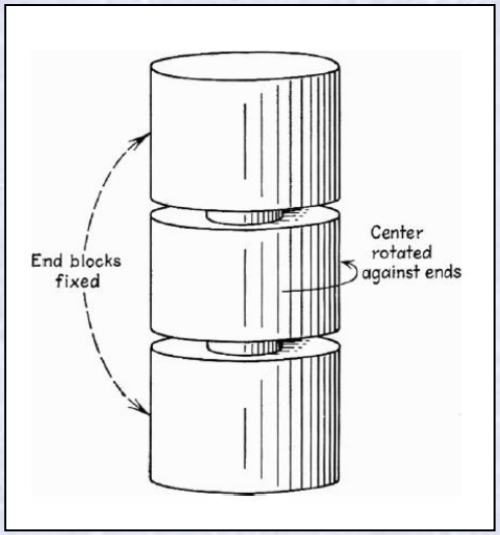

Introduction

High pressure torsion (HPT)

- the strongest grain refinement
- grain size 50 – 150 nm
- limited size: disk shaped samples
  diameter 10 – 20 mm, thickness 0.3 - 0.5 mm

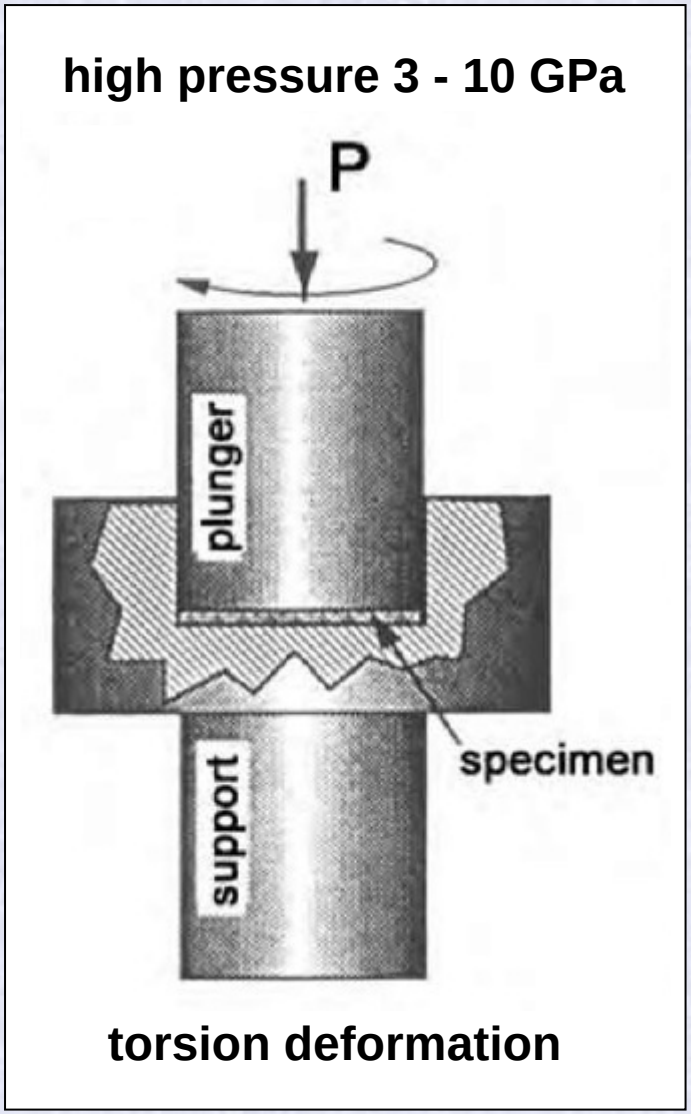

R.Z. Valiev, Nature Materials 3, 511-516 (2004)

Introduction

High pressure torsion (HPT)

- the strongest grain refinement
- grain size 50 – 150 nm

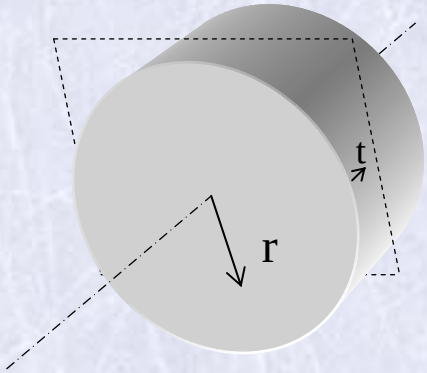

$$e = \ln\left(\vartheta r / l\right)$$

- e - true log. strain
- ϑ - rotation angle
- r - distance from center
- l - sample thickness

high pressure 3 - 10 GPa

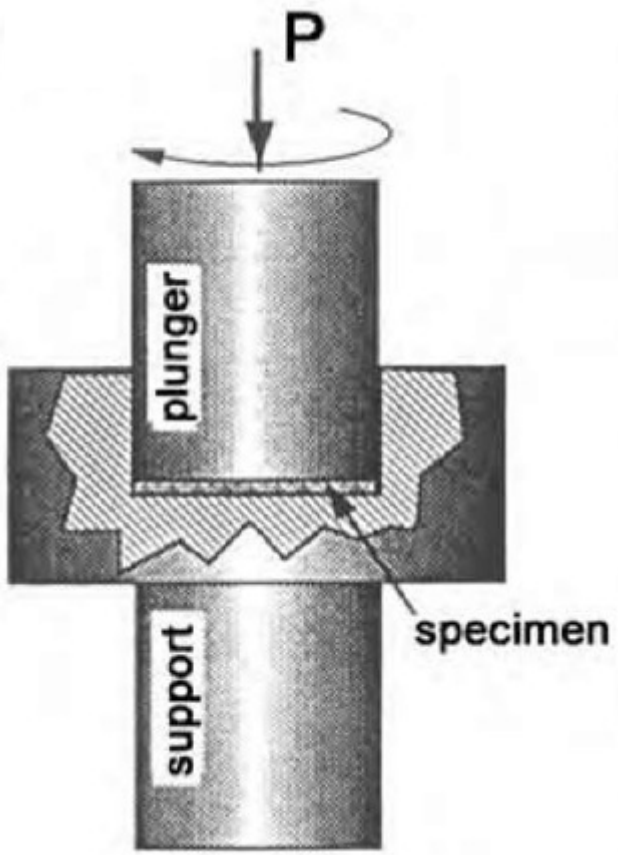

torsion deformation

R.Z. Valiev, Nature Materials 3, 511-516 (2004)

Samples

High pressure torsion (HPT)

- Ufa State Aviation Technical University,
- p = 6 GPa, 5 HPT revolutions
- Cu (99.95%), Al (99.9999%), Fe (99.99%), Ti (99.7%): room temperature
- Nb (99.9%): T = 150^{o}C
- W (99.95%): T = 450^{o}C

Microstructure of UFG metals prepared by SPD

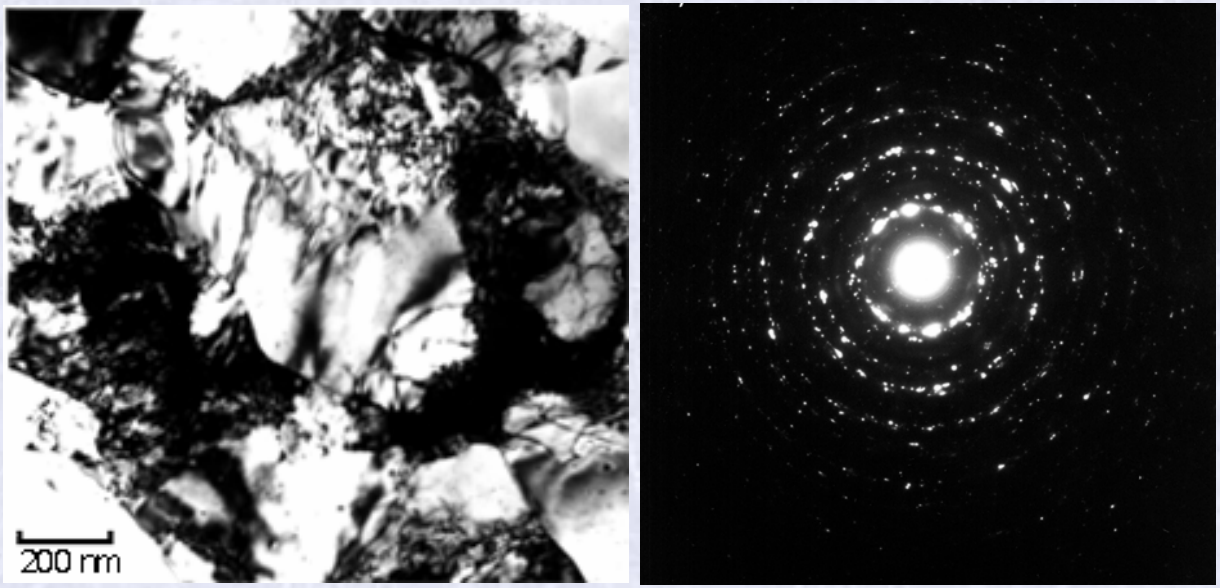

UFG Cu prepared by HPT, p = 6 GPa

- grain size 105(9) nm
- fragmented structure
- high-angle missorientation
- non-equilibrium GB's

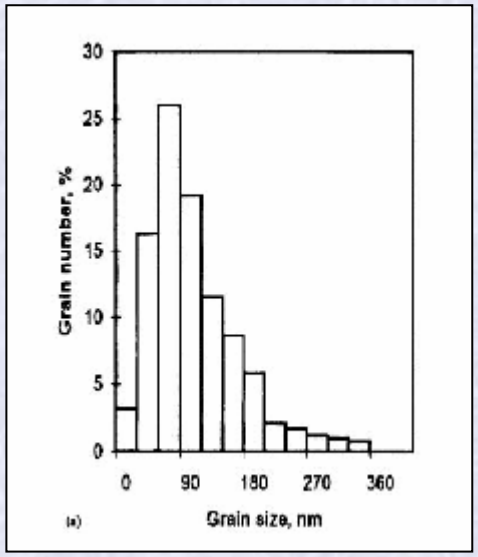

grain size distribution

Microstructure of UFG metals prepared by SPD

polycrystalline material

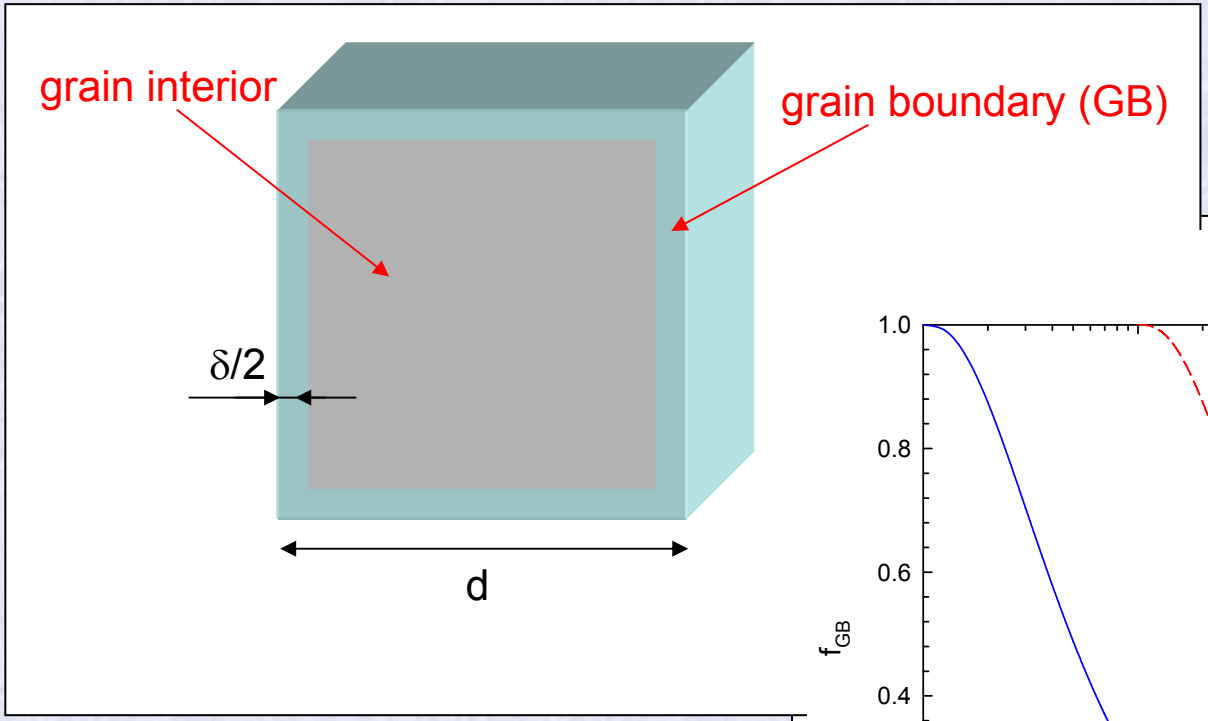

equilibrium GB: $\delta \approx 1$ nm

non-equilibrium GB: $\delta \approx 10$ nm

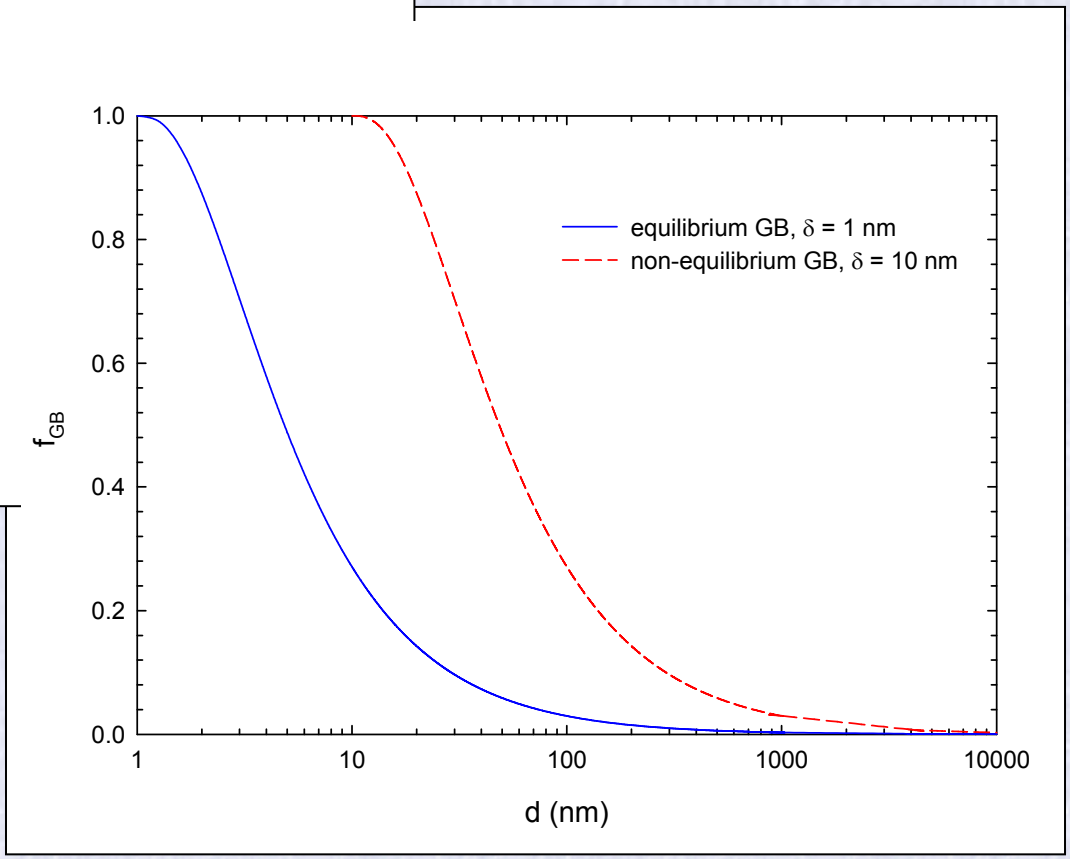

volume fraction of GB's

$$f_{GB} = 1 - \left(\frac{d - \delta}{d} \right)^3$$

Microstructure of UFG metals prepared by SPD

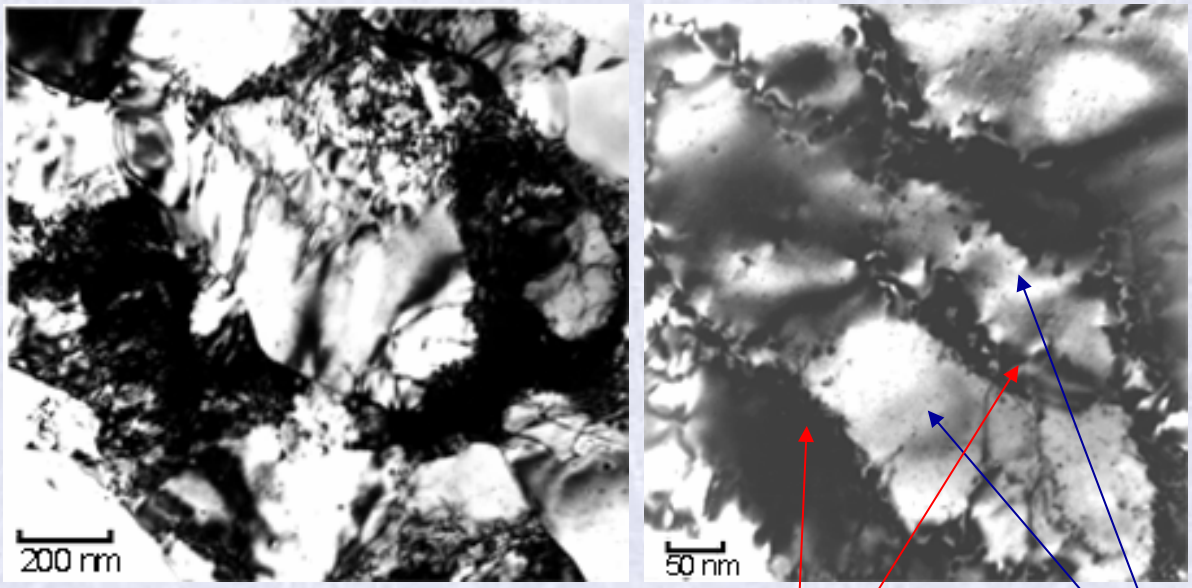

UFG Cu prepared by HPT, p = 6 GPa

distorted regions along GB's - high number of dislocations
- thickness δ ~ 10 nm

grain interiors almost free of dislocations

- grain size 105(9) nm
- fragmented structure
- high-angle missorientation
- non-equilibrium GB's

Generation of vacancies during SPD

movement of dislocation with jogs

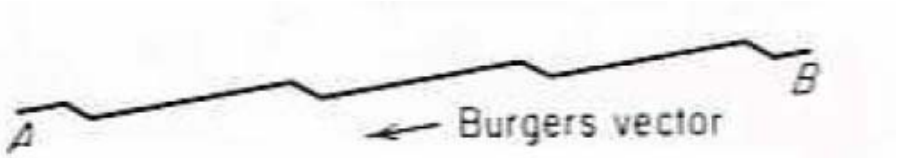

1. no stress

Generation of vacacies during SPD

movement of dislocation with jogs

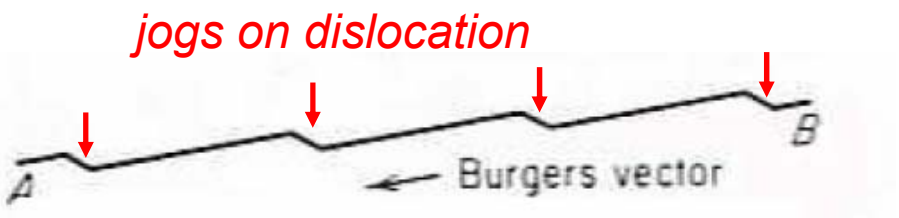

1. no stress

Generation of vacancies during SPD

movement of dislocation with jogs

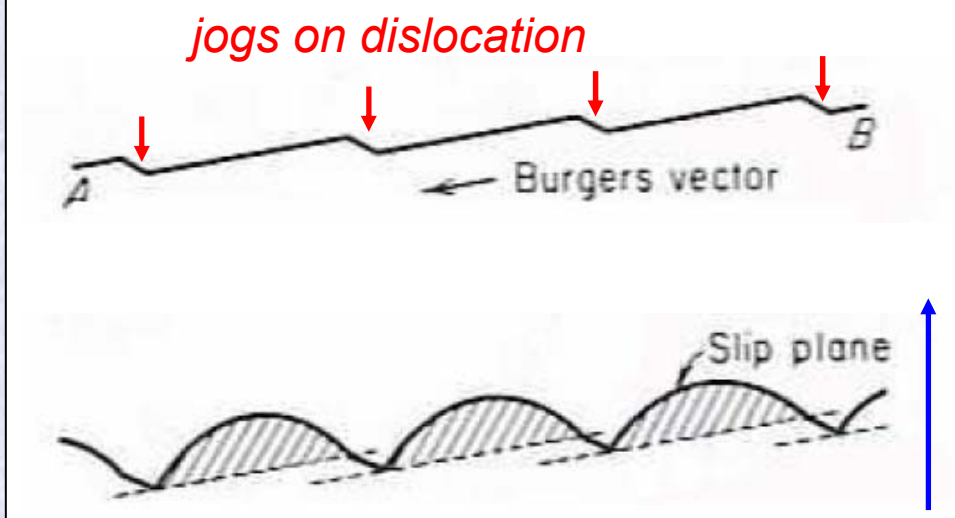

1. no stress

2. applied stress

Generation of vacancies during SPD

movement of dislocation with jogs

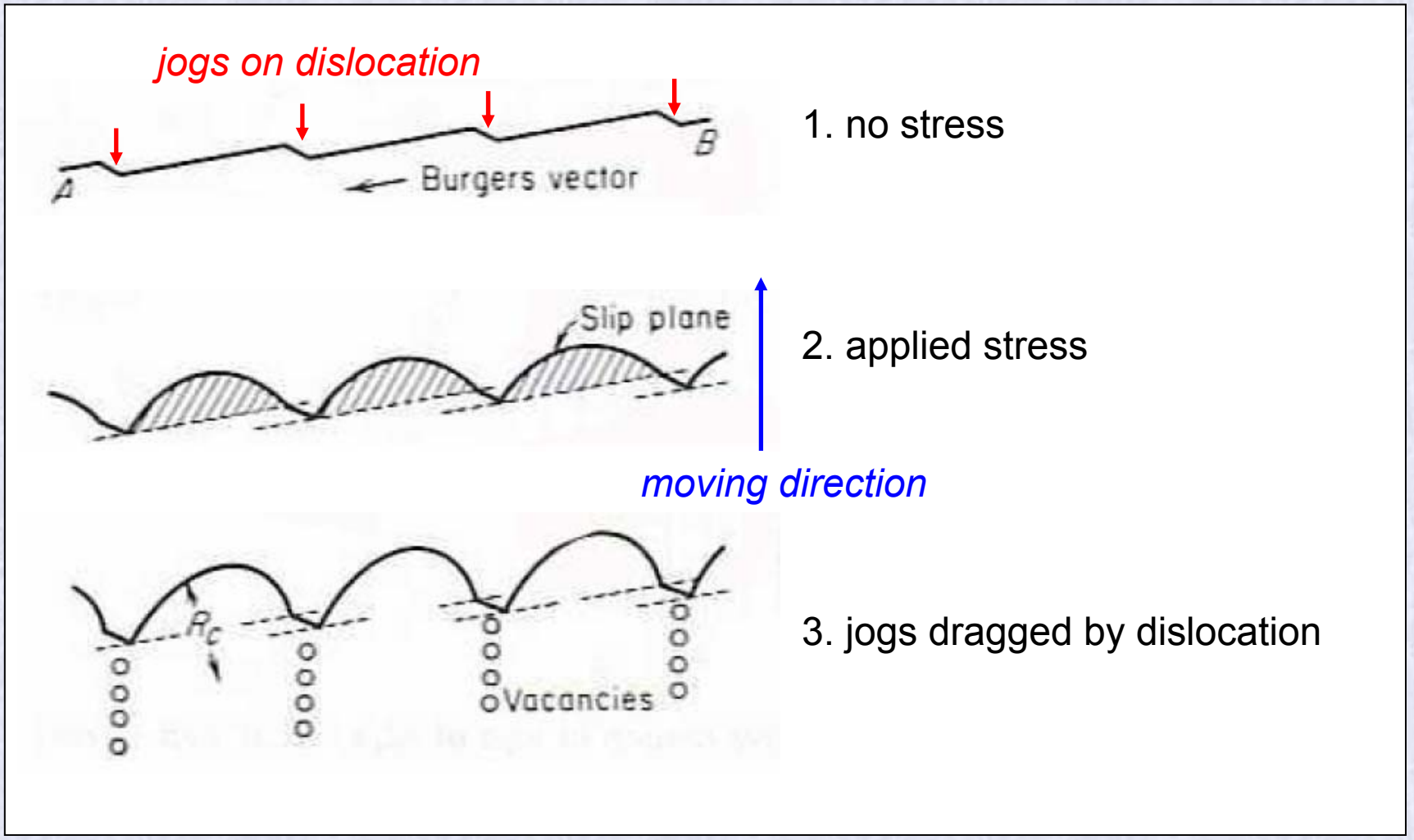

Generation of vacacies during SPD

- **X-ray line profile analyzis:**
  - dislocation density $\rho_D \approx 10^{14} – 10^{15}$ m^{-2}

    T. Ungár et al. Mater. Sci. Eng. A 462, 398 (2007)

- **differential scanning calorimetry (DSC) & electrical resistivity**
  - dislocation density $\rho_D \approx 10^{15} – 10^{16}$ m^{-2}

    E. Schafler et al. Mater. Sci. Eng. A 410-411, 169 (2005)

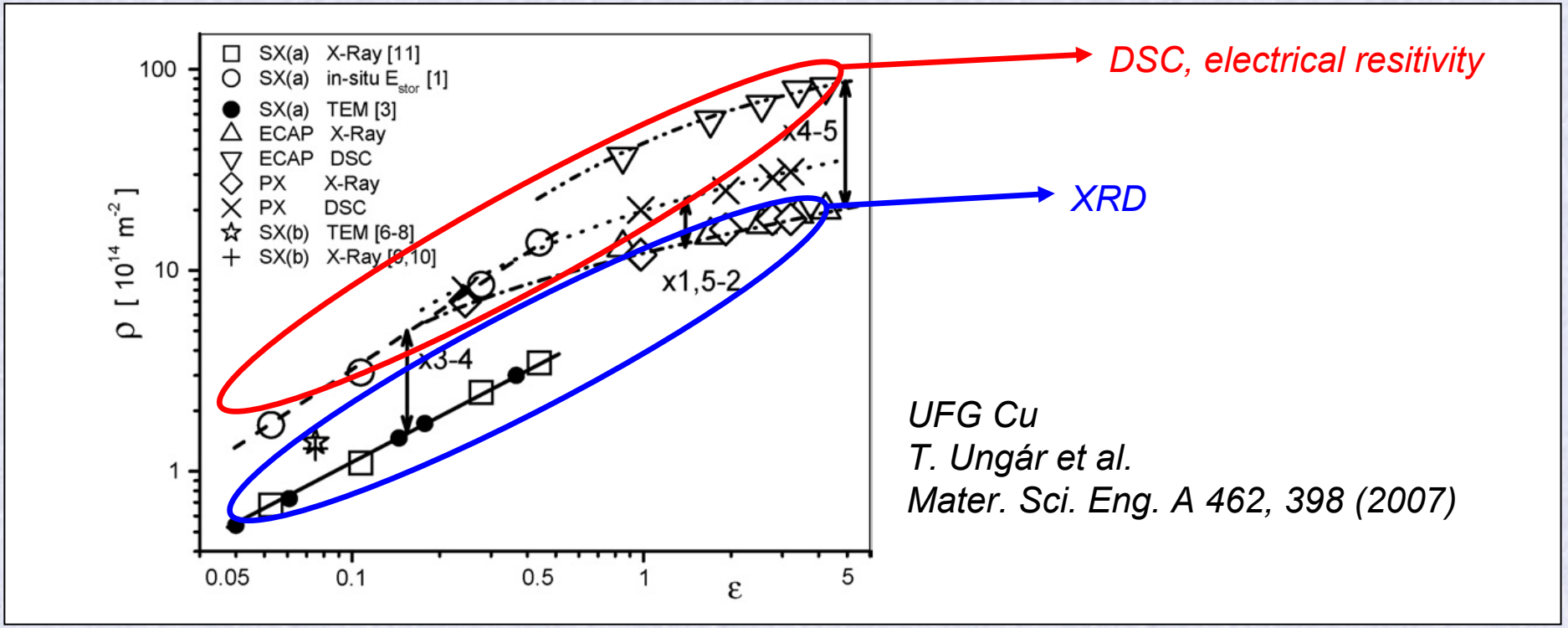

Generation of vacancies during SPD

deformation-induced vacancies contribute to the total stored energy and electrical resitivity, but do not cause broadening of XRD profiles

- **indirect evidence for deformation-induced vacancies**

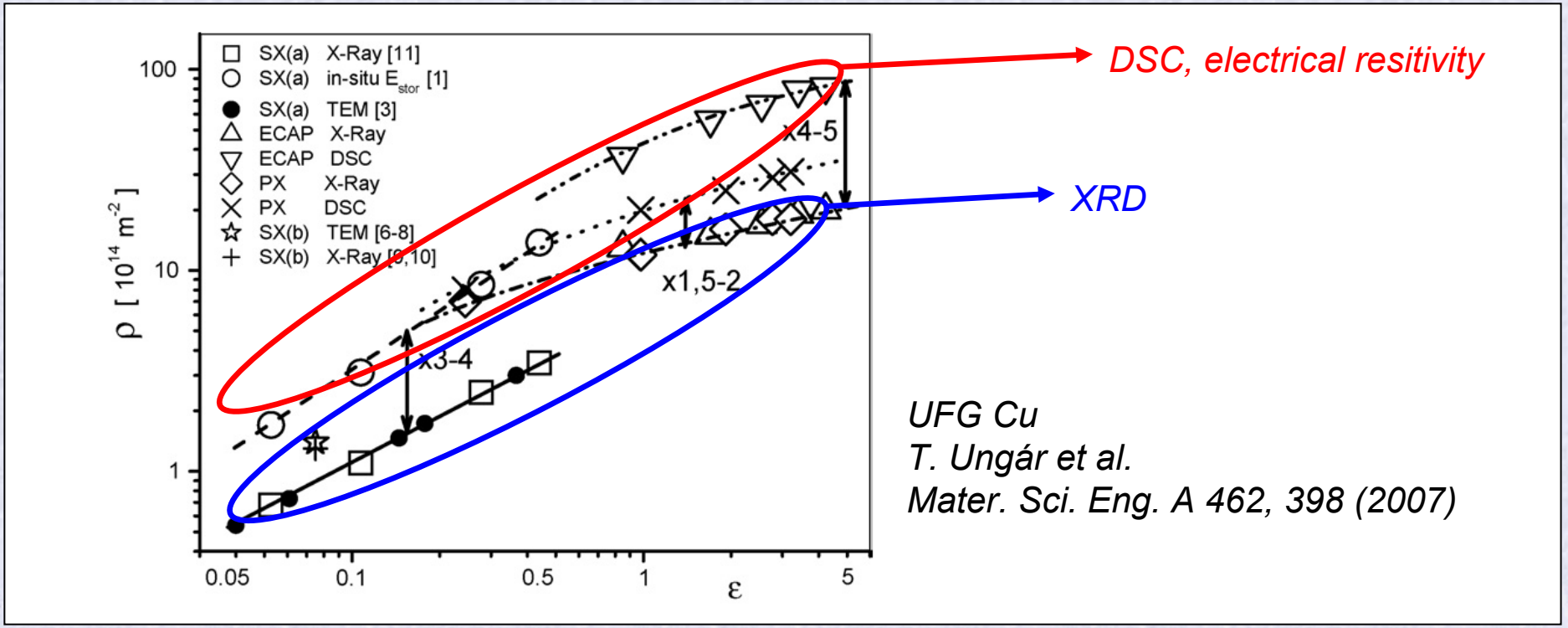

Generation of vacacies during SPD

- **positron annihilation spectroscopy (PAS)**

↓

- **direct evidence for deformation-induced vacancies**

- **Vacancies introduced by SPD agglomerate and form vacancy clusters.**

UFG Cu: J. Čížek et al. Acta Mater. 59, 2322 (2011)
UFG Cu,Ni: B. Oberdorfer et al. Phys. Rev. Lett. 105, 146101 (2010)

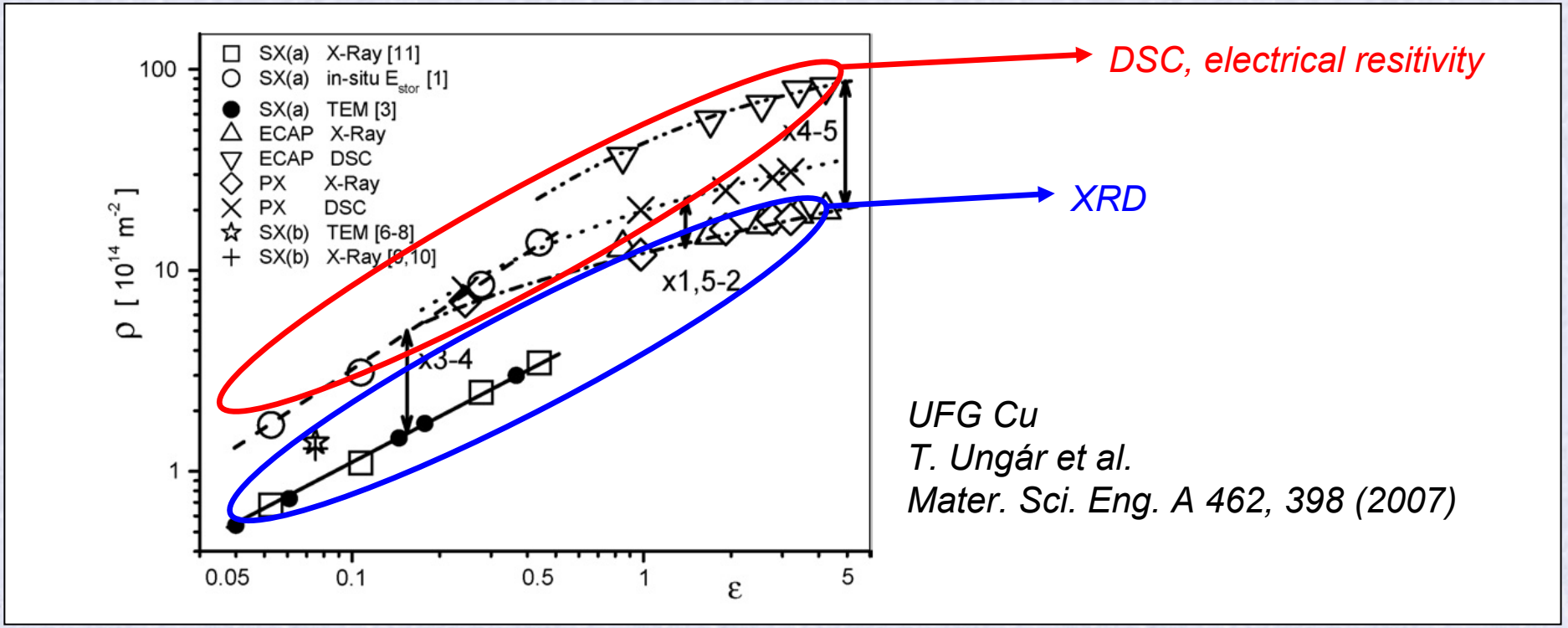

LT spectroscopy

Digital LT spectrometer: *F. Bečvář et al., Nucl. Instr. Meth. A **539**, 372 (2005)*

- Two photomultipliers Hamamatsu H3378
- BaF_2 scintilators truncated cone (∅ 18-36 mm, thickness 12 mm)
- two 8-bit digitizers Acqiris DC211, sampling rate 4 GHz
- time resolution 145 ps (FWHM ^{22}Na)
- at least 10^7 annihilation events collected in each LT spectrum

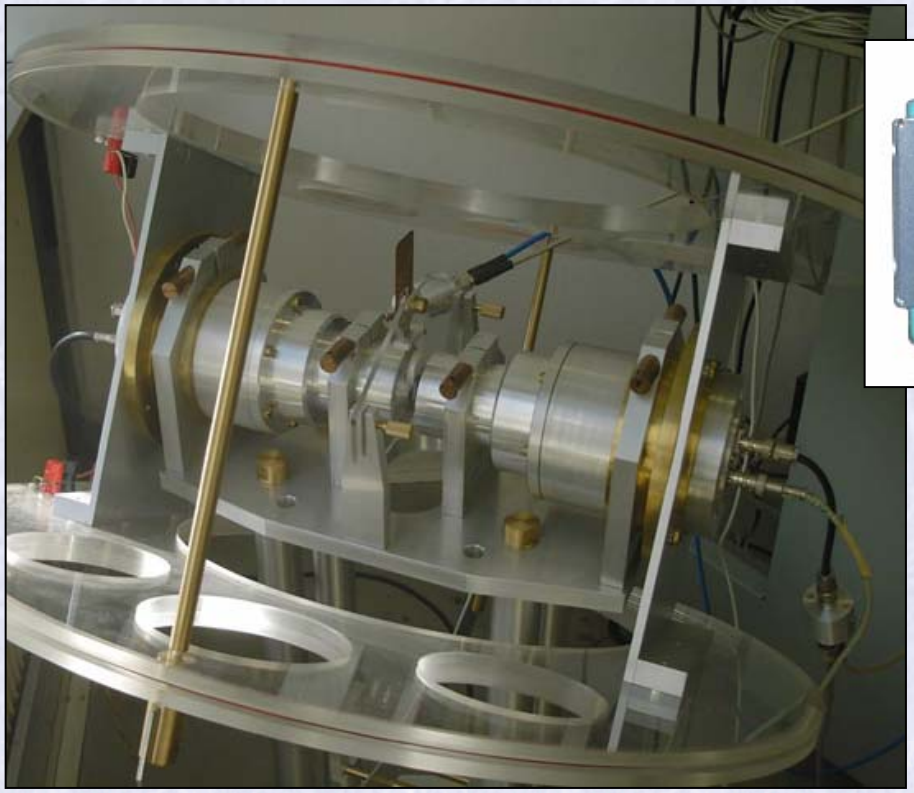

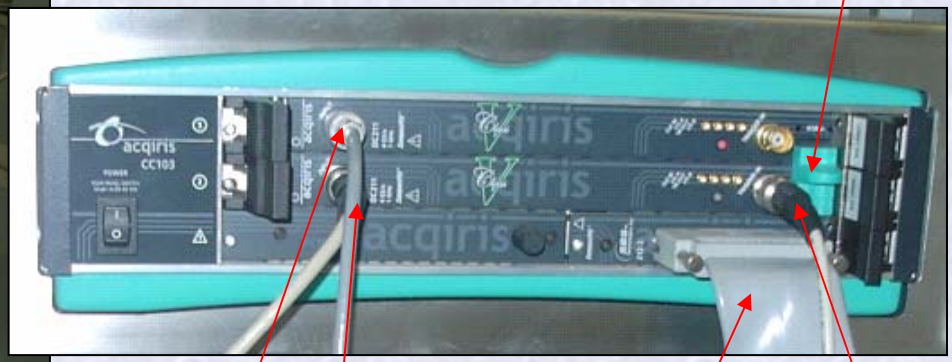

Positron lifetime studies of UFG metals prepared by SPD

- HPT, p = 6 GPa, 5 HPT revolutions
- measured in the centre of the sample disk

sample	τ_1 (ps)	I_1 (%)	τ_2 (ps)	I_2 (%)	τ_3 (ps)	I_3 (%)
Cu, fcc	-	-	164(1)	76.0(6)	256(2)	24.0(5)
Al, fcc	149(8)	71(5)	252(9)	26(1)	450(50)	3(1)
Fe, bcc	-	-	150.8(6)	91.1(4)	360(9)	8.9(4)
Nb, bcc	-	-	173.9(8)	94(1)	300(10)	6(1)
W, bcc	-	-	160.8(6)	90.8(4)	367(7)	9.2(7)
Ti, hcp	-	-	185.2(5)	98.4(7)	430(70)	1.6(7)

free positrons dislocations vacancy clusters

Ab-initio theoretical calculations of positron parameters

Standard scheme:

J. Puska, R. Nieminen, J. Phys. F: Met. Phys. 13, 333 (1983)

- electron density – atomic superposition (ATSUP) $n_-(\mathbf{r}) = \sum_i n_-^{\mathrm{at}}\left(\left|\mathbf{r} - \mathbf{R}_i\right|\right)$
- limit of vanishing positron density
- positron lifetime: $\tau^{-1} = \pi r_e^2 c \int d\mathbf{r} \left|\psi^+(\mathbf{r})\right|^2 n_-(\mathbf{r}) \gamma\left[n_-(\mathbf{r})\right]$
- electron-positron correlation – LDA approach

  E. Boroński and R. Nieminen, Phys. Rev. B 3820, 34 (1986)

- 512 atom-based supercells
- fcc metals (Al, Cu), bcc metals (Fe, Nb, W), hcp metals (Mg, Ti)
- equilibrium geometry of cluster $\rightarrow$ minimum surface area
- ionic relaxations not considered

Theoretical calculations – bcc metals

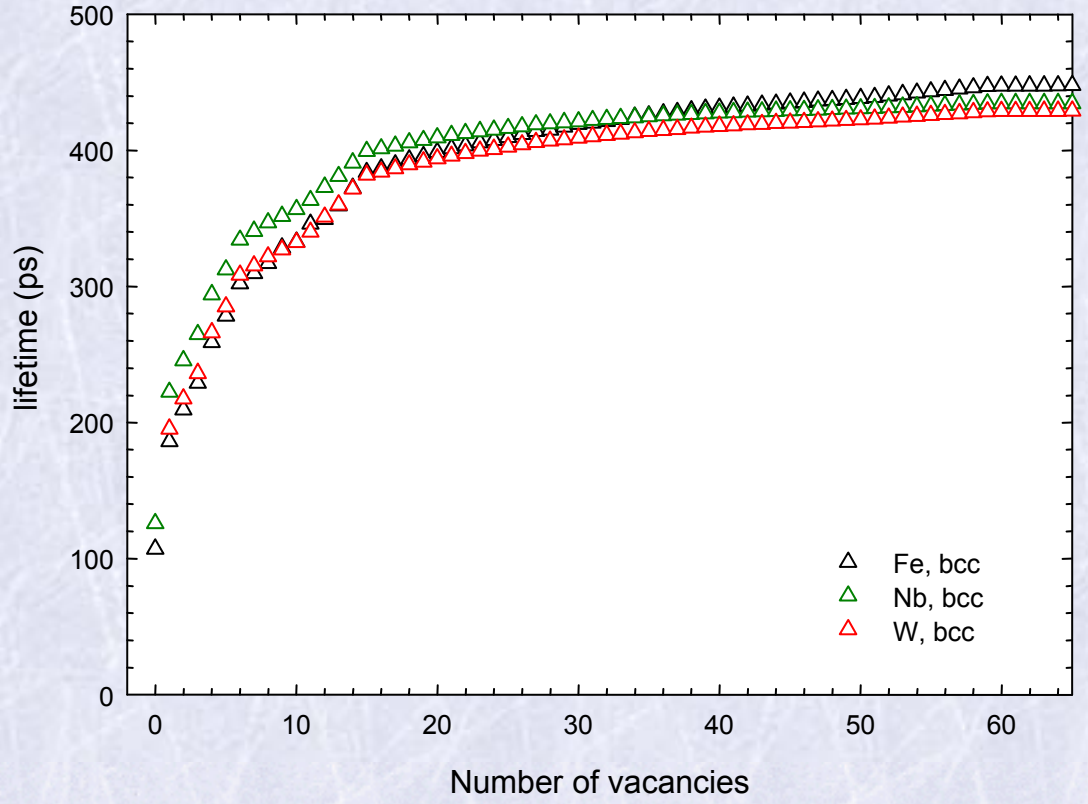

Theoretical calculations – bcc metals

6V cluster

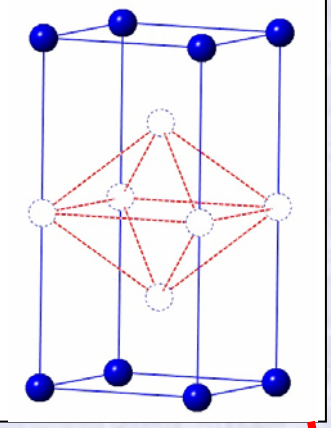

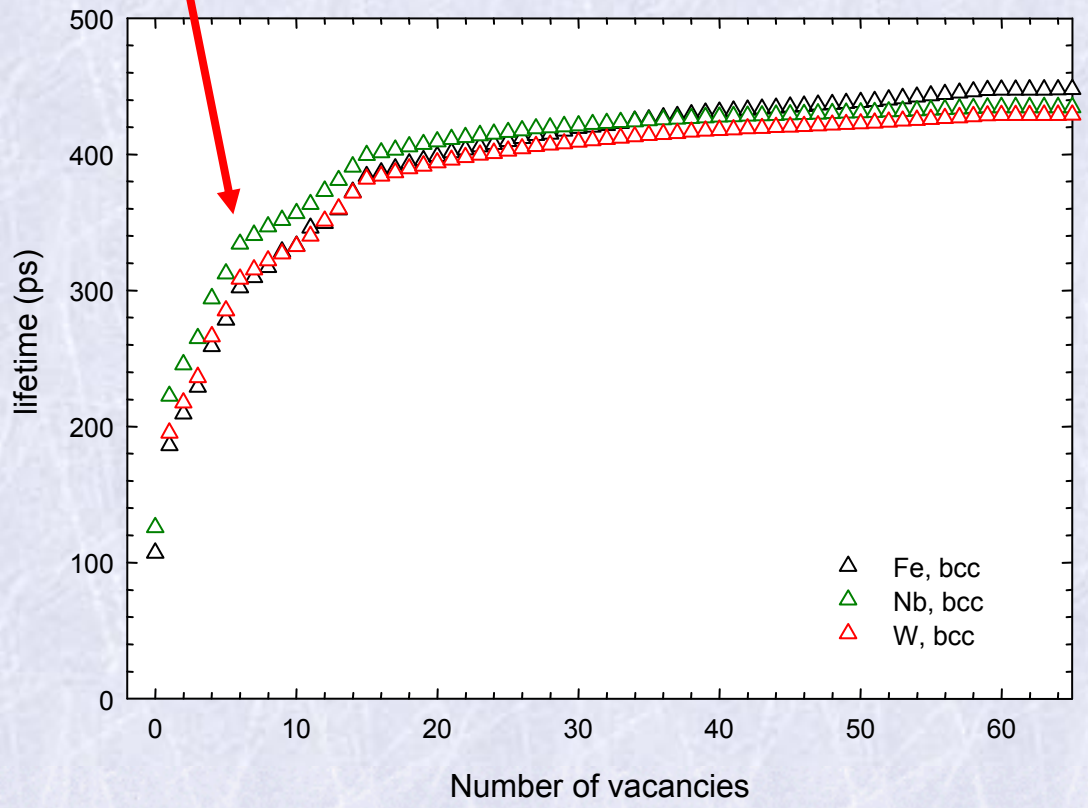

Theoretical calculations – bcc metals

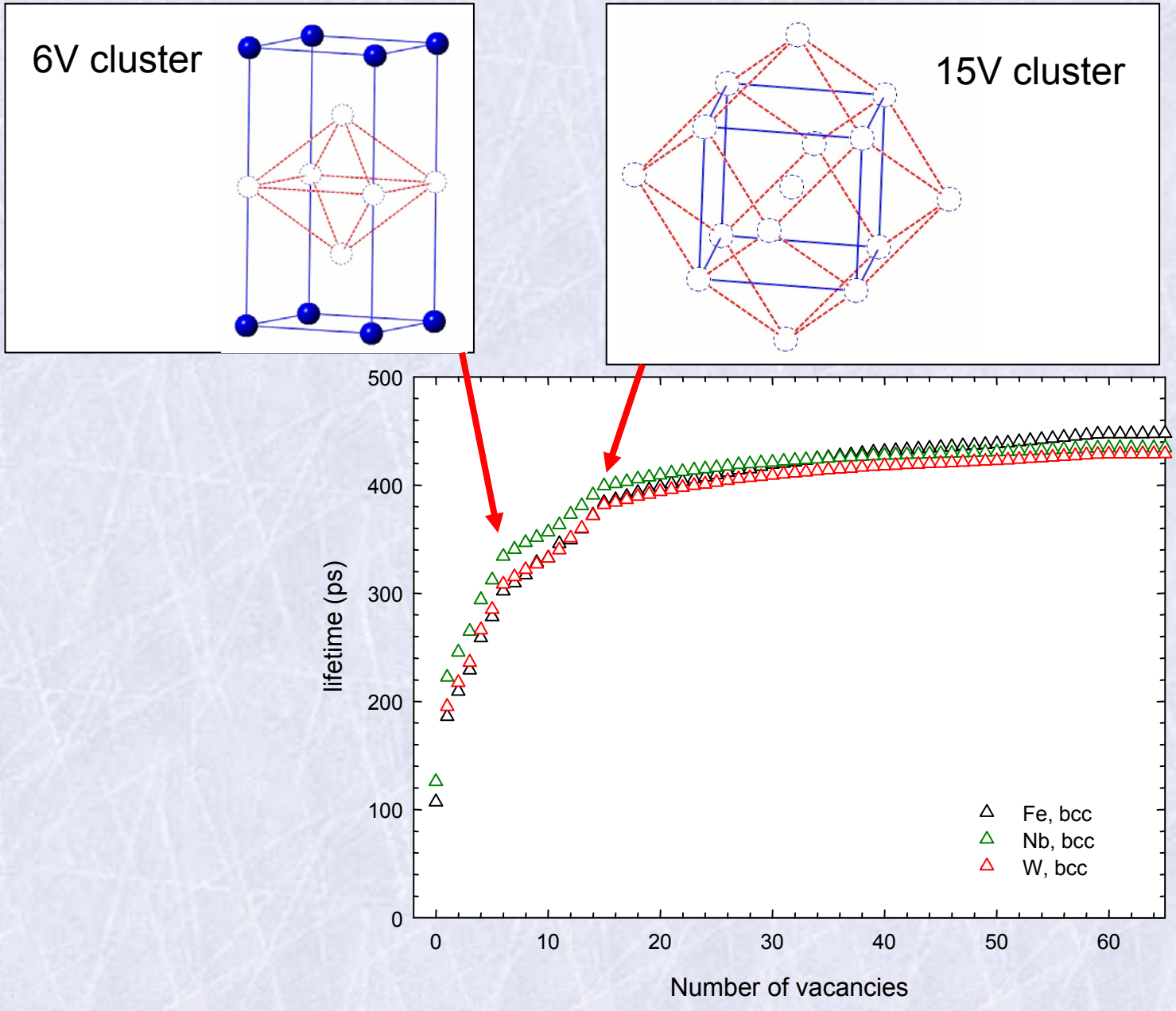

Theoretical calculations – fcc metals

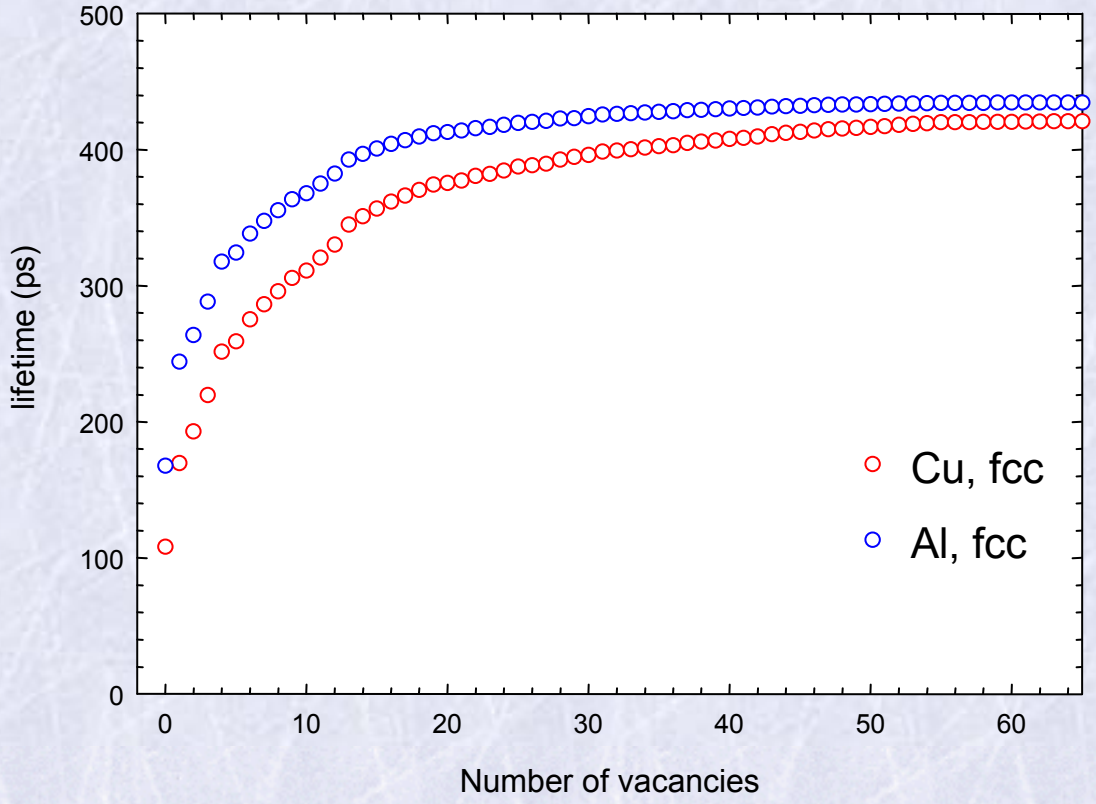

Theoretical calculations – fcc metals

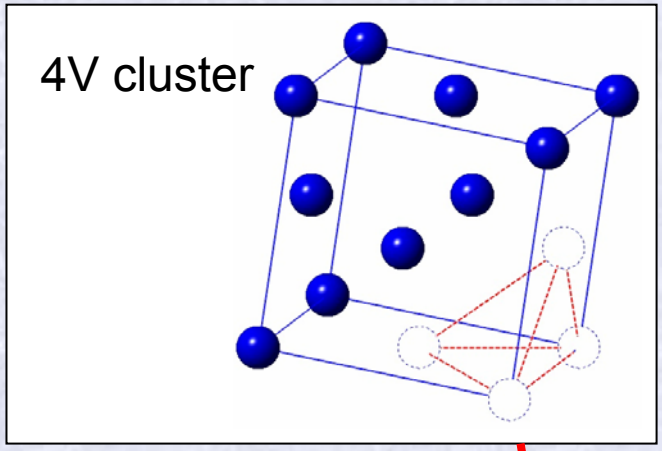

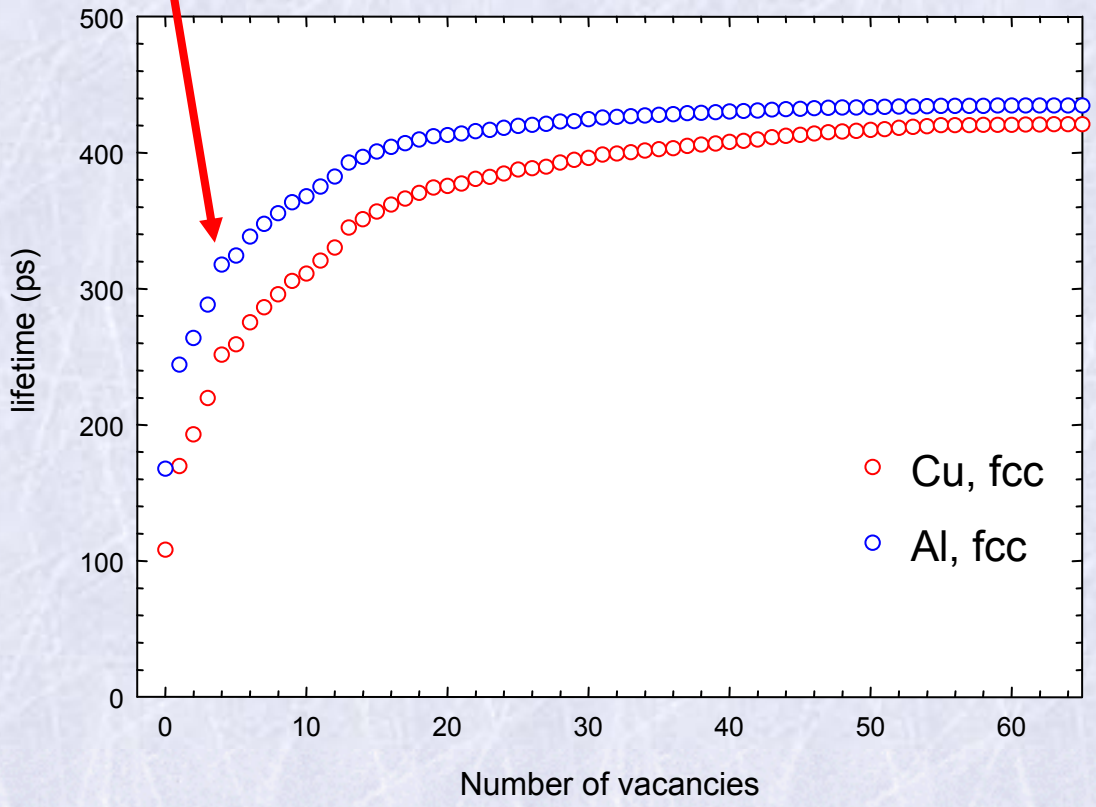

Theoretical calculations – fcc metals

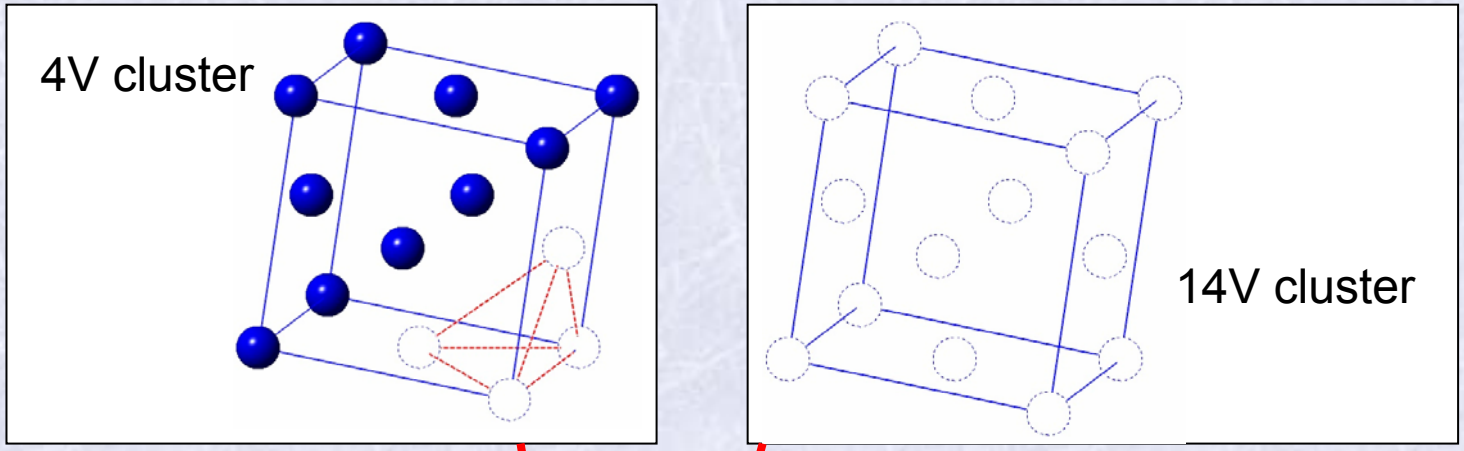

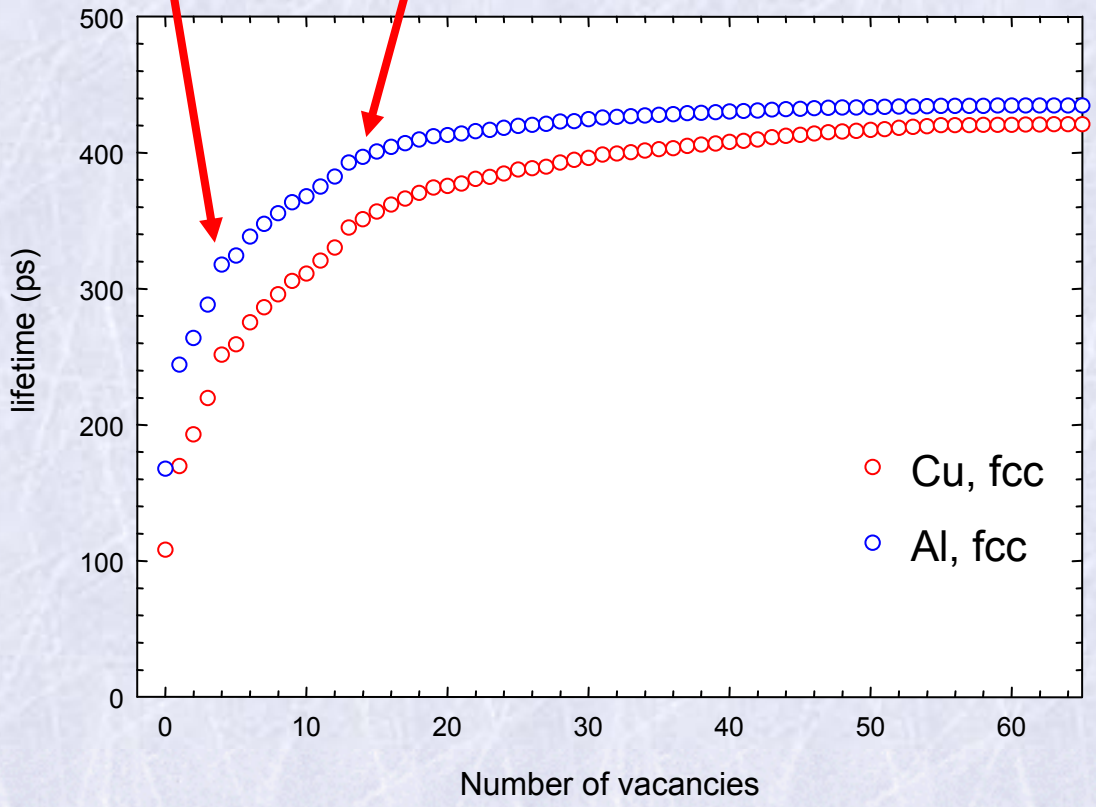

Theoretical calculations – hcp metals

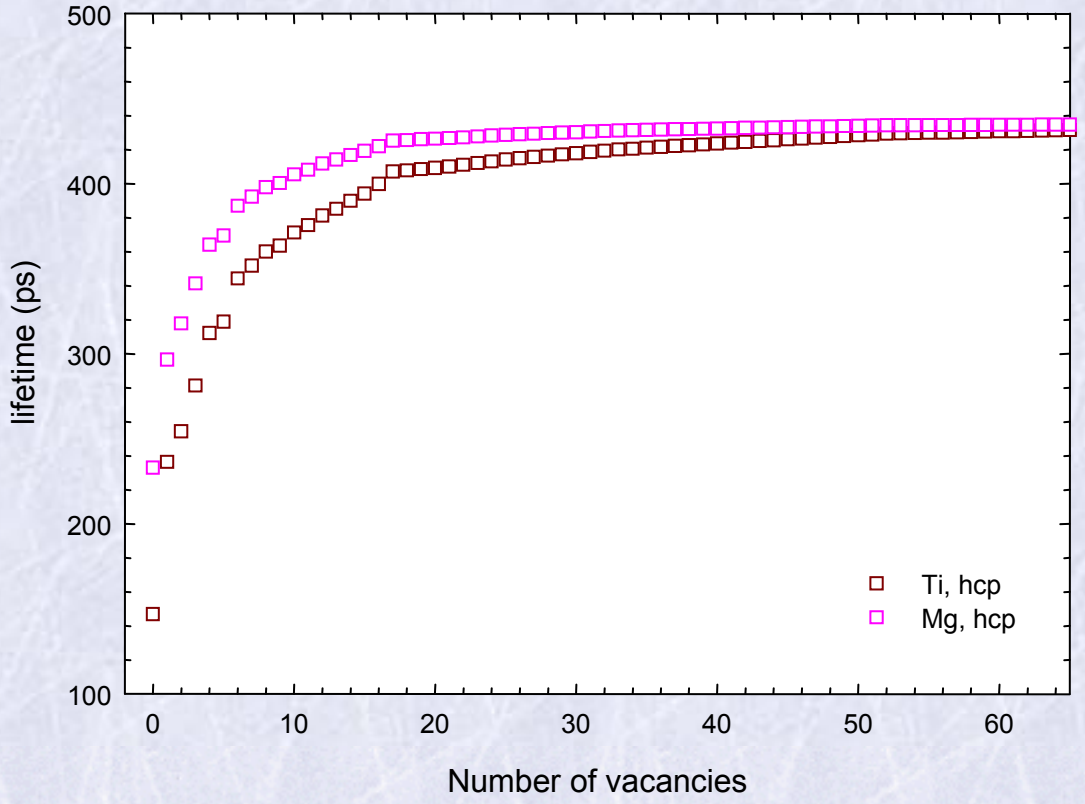

Theoretical calculations – hcp metals

4V cluster

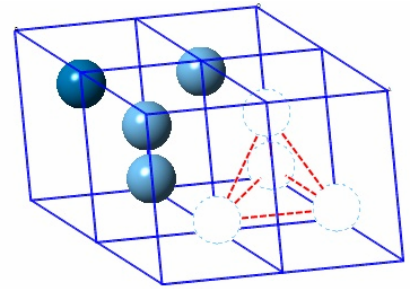

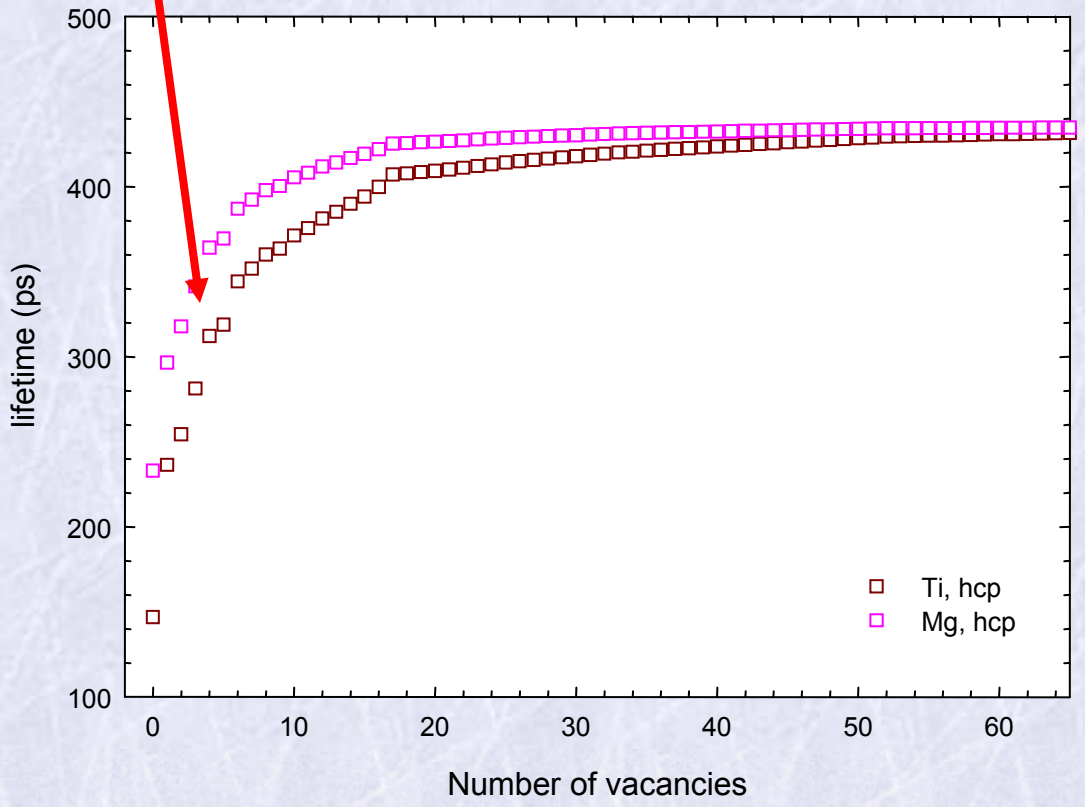

Theoretical calculations – hcp metals

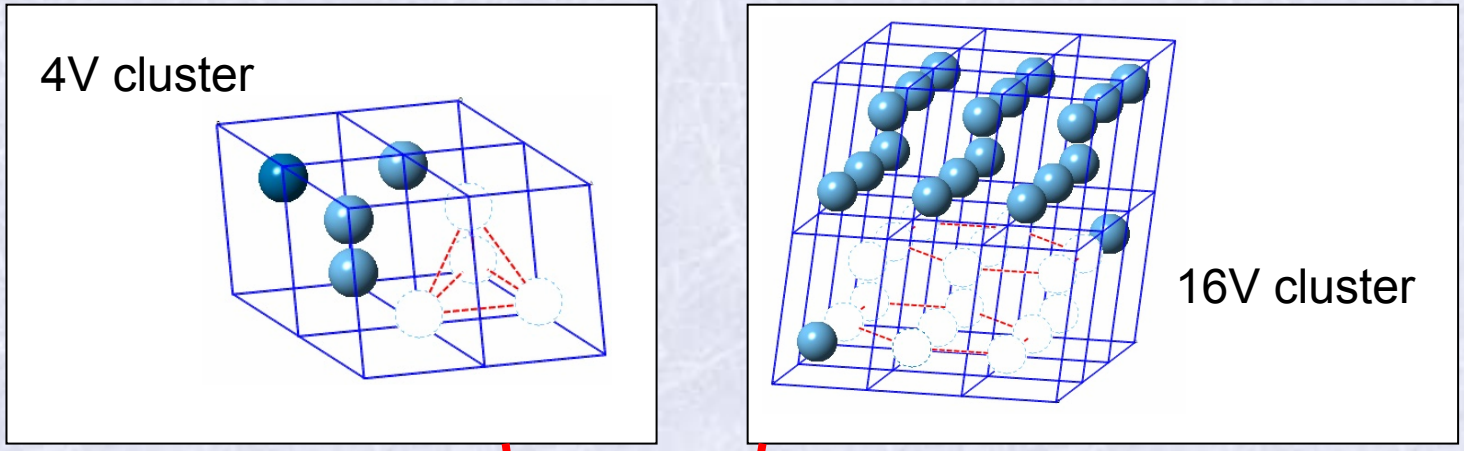

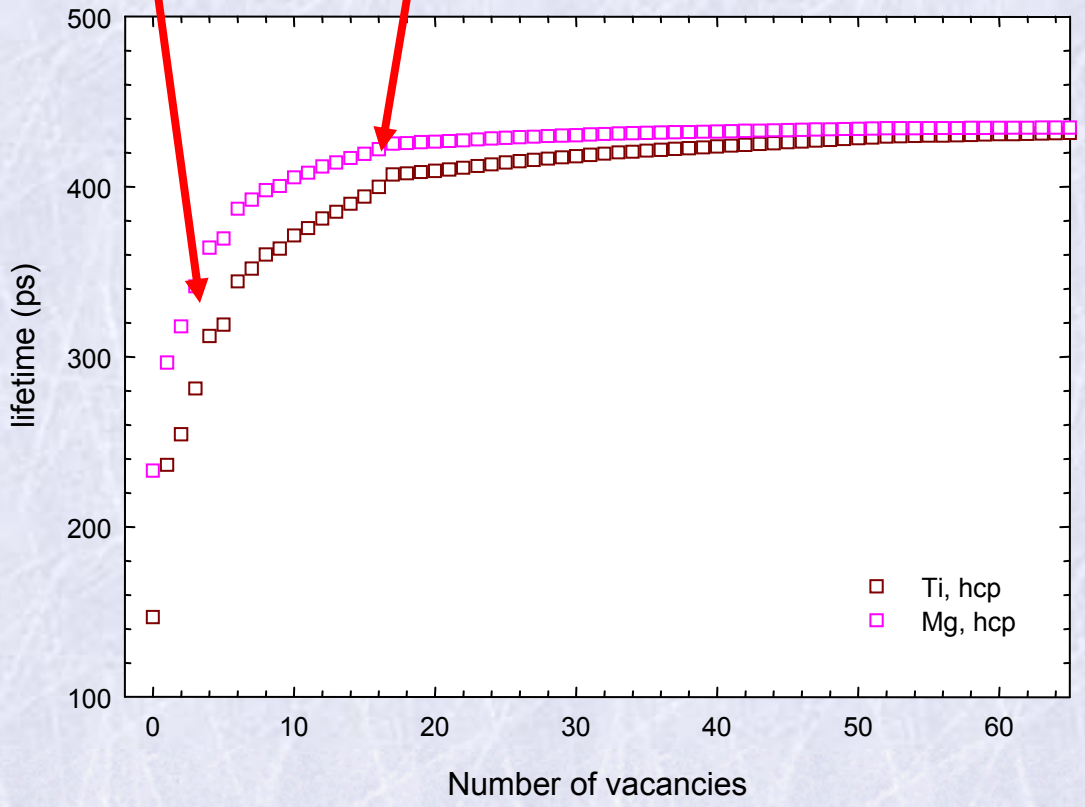

Decomposition of positron lifetime spectrum

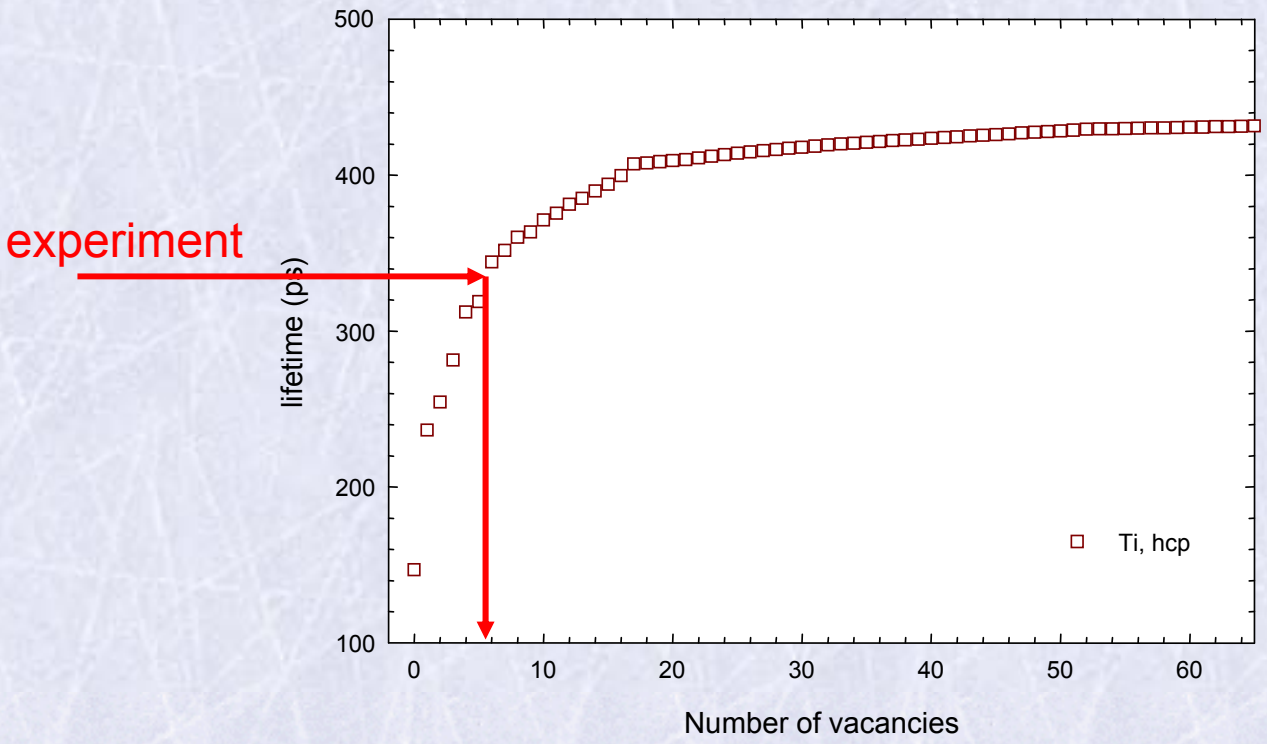

Decomposition of positron lifetime spectrum

- **traditional approach:** sum of discreet components

$$S(t) = \left(\sum_{i=1}^{n} \frac{I_i}{\tau_i} e^{-\frac{t}{\tau_i}} \right) \otimes R(t) + B \qquad \sum_{i=1}^{n} I_i = 1$$

resolution function

random background

experiment

τ_i

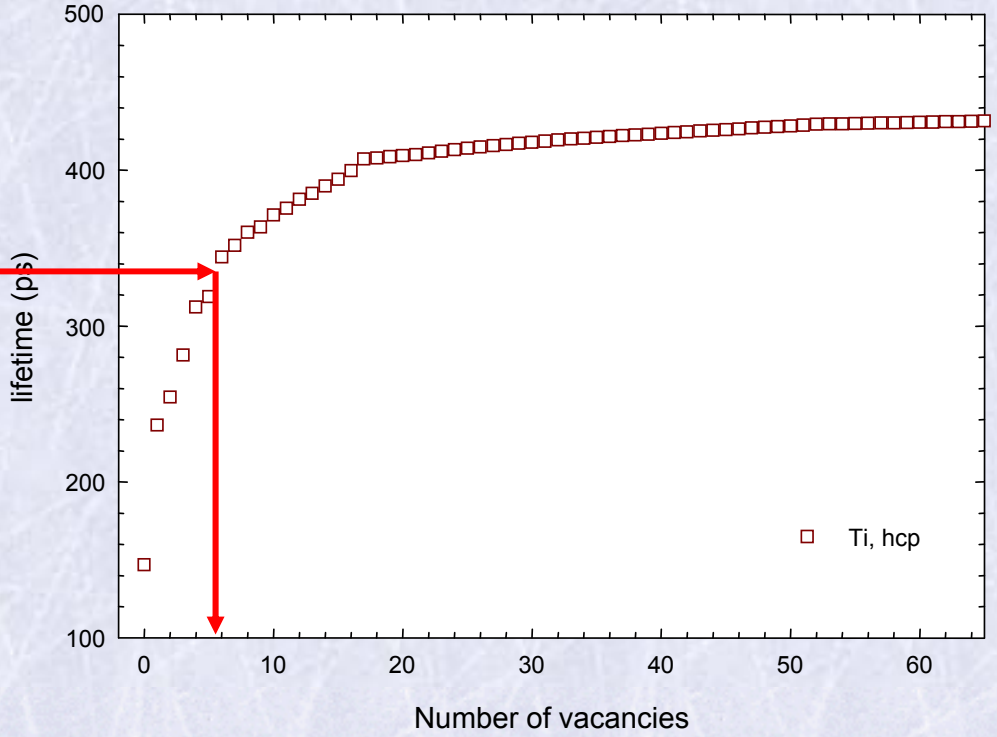

Decomposition of positron lifetime spectrum

- **traditional approach:** sum of discreet components

$$S(t) = \left(\sum_{i=1}^{n} \frac{I_i}{\tau_i} e^{-\frac{t}{\tau_i}} \right) \otimes R(t) + B \qquad \sum_{i=1}^{n} I_i = 1$$

- **new approach:** discreet components + cluster distribution

$$S(t) = \left(\sum_{i=1}^{n-1} \frac{I_i}{\tau_i} e^{-\frac{t}{\tau_i}} + I_d \left(\sum_{N=1}^{N_{\max}} \nu_N \right)^{-1} \sum_{N=1}^{N_{\max}} \frac{P(N)\nu_N}{\tau_N} e^{-\frac{t}{\tau_N}} \right) \otimes R(t) + B \qquad \sum_{i=1}^{n-1} I_i + I_d = 1$$

discreet components

- dislocations,

- free positrons (if any)

cluster contribution

Decomposition of positron lifetime spectrum

- **cluster contribution**

$$I_d\left(\sum_{N=1}^{N_{\max}}\nu_N\right)^{-1}\sum_{N=1}^{N_{\max}}\frac{P(N)\nu_N}{\tau_N}e^{-\frac{t}{\tau_N}}$$

τ_N - positron lifetime for cluster consting of *N* vacancies

- obtained from theoretical calculations

- each component is weighted by a factor $P(N)\nu_N$

ν_N - the specific positron trapping rate for a cluster consting of *N* vacancies

$P(N)$ - the relative population of clusters consting of *N* vacancies

Specific positron trapping rate for vacancy clusters ν_N

- accounts for cross-section for positron trapping increasing with cluster size
- small clusters ($N \leq 10$): $\nu_N \sim N$
- larger clusters ($N > 10$): ν_N gradually saturates

R. M. Nieminen, J. Laakkonen, Appl. Phys.20, 181 (1979)

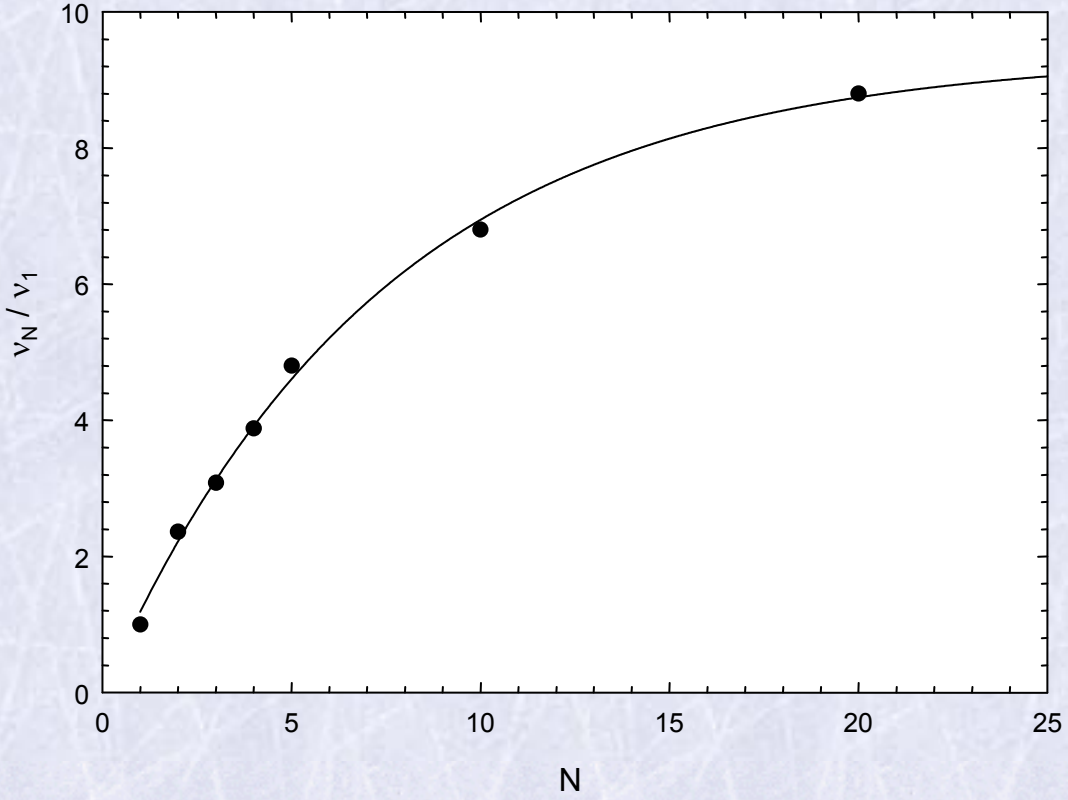

$$\nu_N / \nu_1 \approx a\left(1 - e^{-bN}\right)$$

$$a = 9.4$$

$$b = 0.13$$

Size distribution of vacancy clusters

- movement of dislocation with a jog

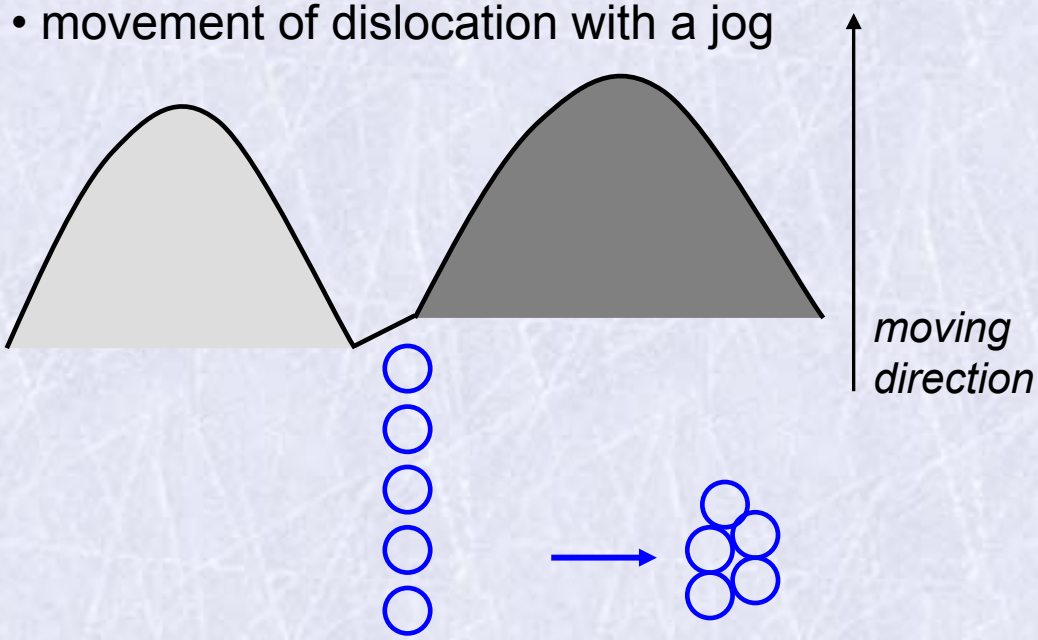

- many attempts to move a jog under the applied stress

↓

- **Poisson distribution**

$$P(N) = \frac{\nu_d{}^N e^{-\nu_d}}{N!} \qquad \sum_{N=1}^{N_{\max}} P(N) = 1$$

- the mean size of vacancy cluster: ν_d

Decomposition of positron lifetime spectrum

- **traditional approach:** sum of discreet components

$$S(t) = \left(\sum_{i=1}^{n} \frac{I_i}{\tau_i} e^{-\frac{t}{\tau_i}} \right) \otimes R(t) + B \qquad \sum_{i=1}^{n} I_i = 1$$

- **new approach:** discreet components + cluster distribution

$$S(t) = \left(\sum_{i=1}^{n-1} \frac{I_i}{\tau_i} e^{-\frac{t}{\tau_i}} + I_d \left(\sum_{N=1}^{N_{\max}} \nu_N \right)^{-1} \sum_{N=1}^{N_{\max}} \frac{\nu_d^N e^{-\nu_d} \nu_N}{N! \tau_N} e^{-\frac{t}{\tau_N}} \right) \otimes R(t) + B \quad \sum_{i=1}^{n-1} I_i + I_d = 1$$

- the only fitting parameters related to cluster contribution are I_d and ν_d (for Poisson distribution the mean equals the variance)

- the new approach contains the *same number* of fitting parameters as the traditional approach

Decomposition of positron lifetime spectrum

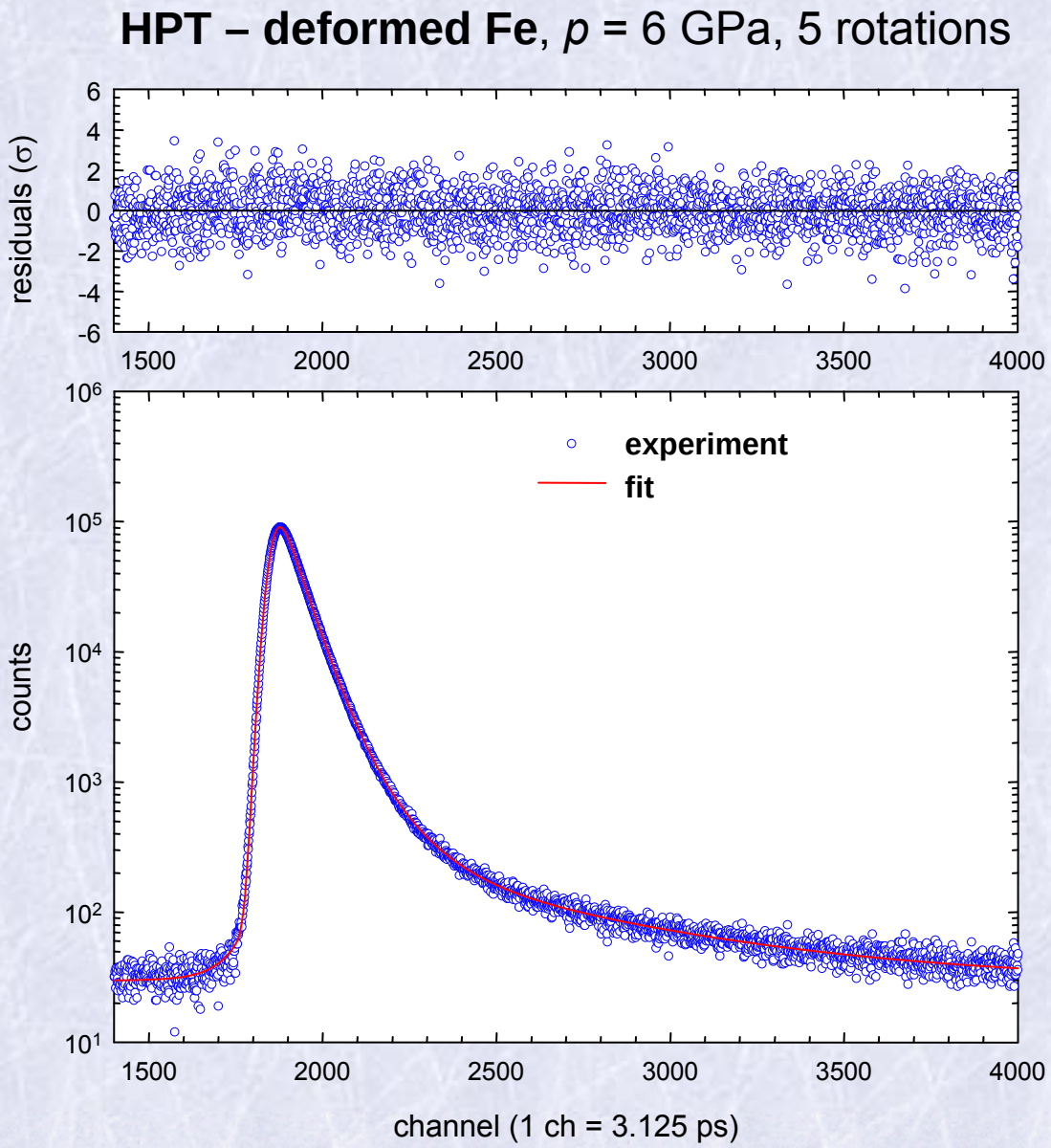

Decomposition of positron lifetime spectrum

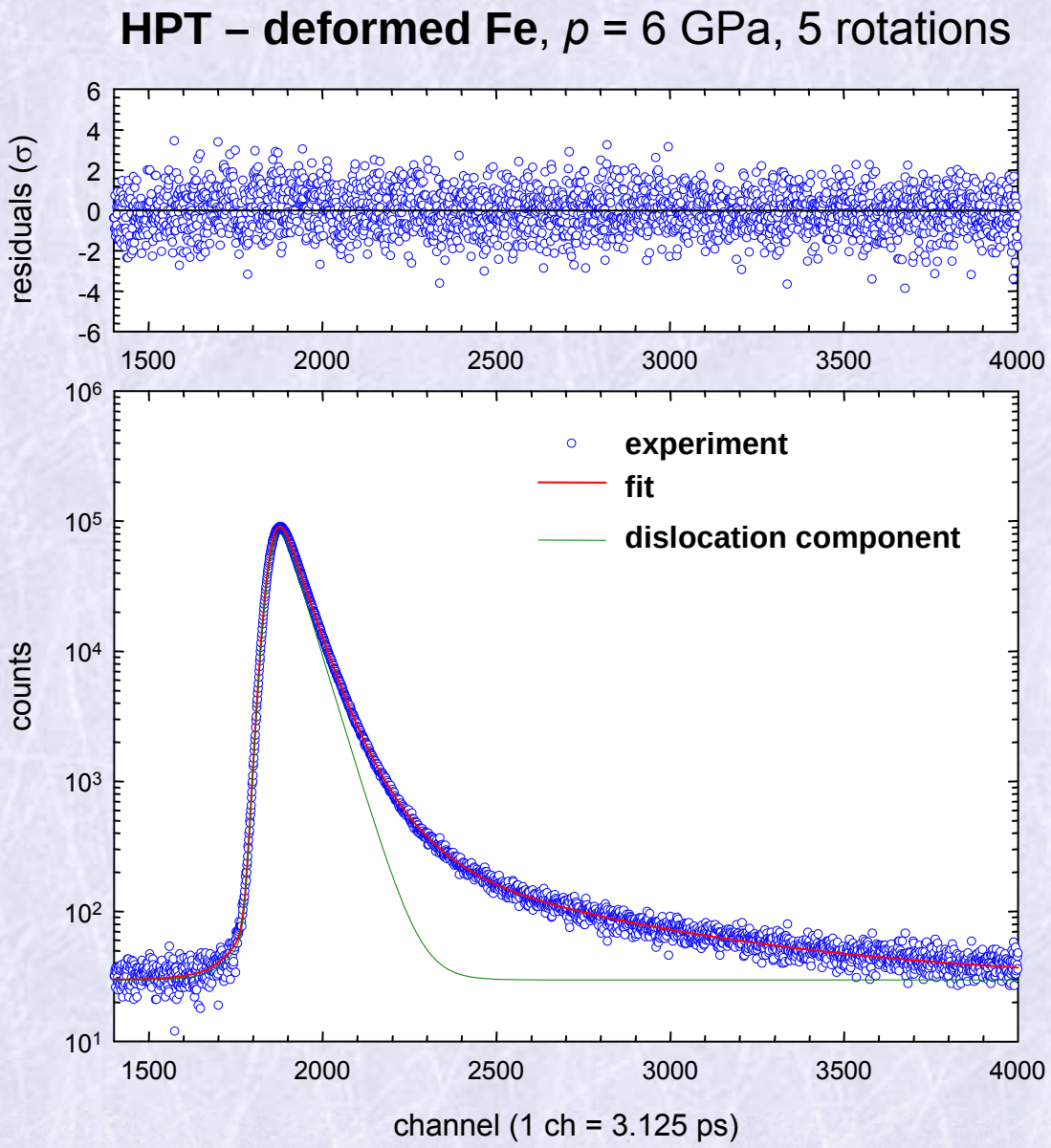

Decomposition of positron lifetime spectrum

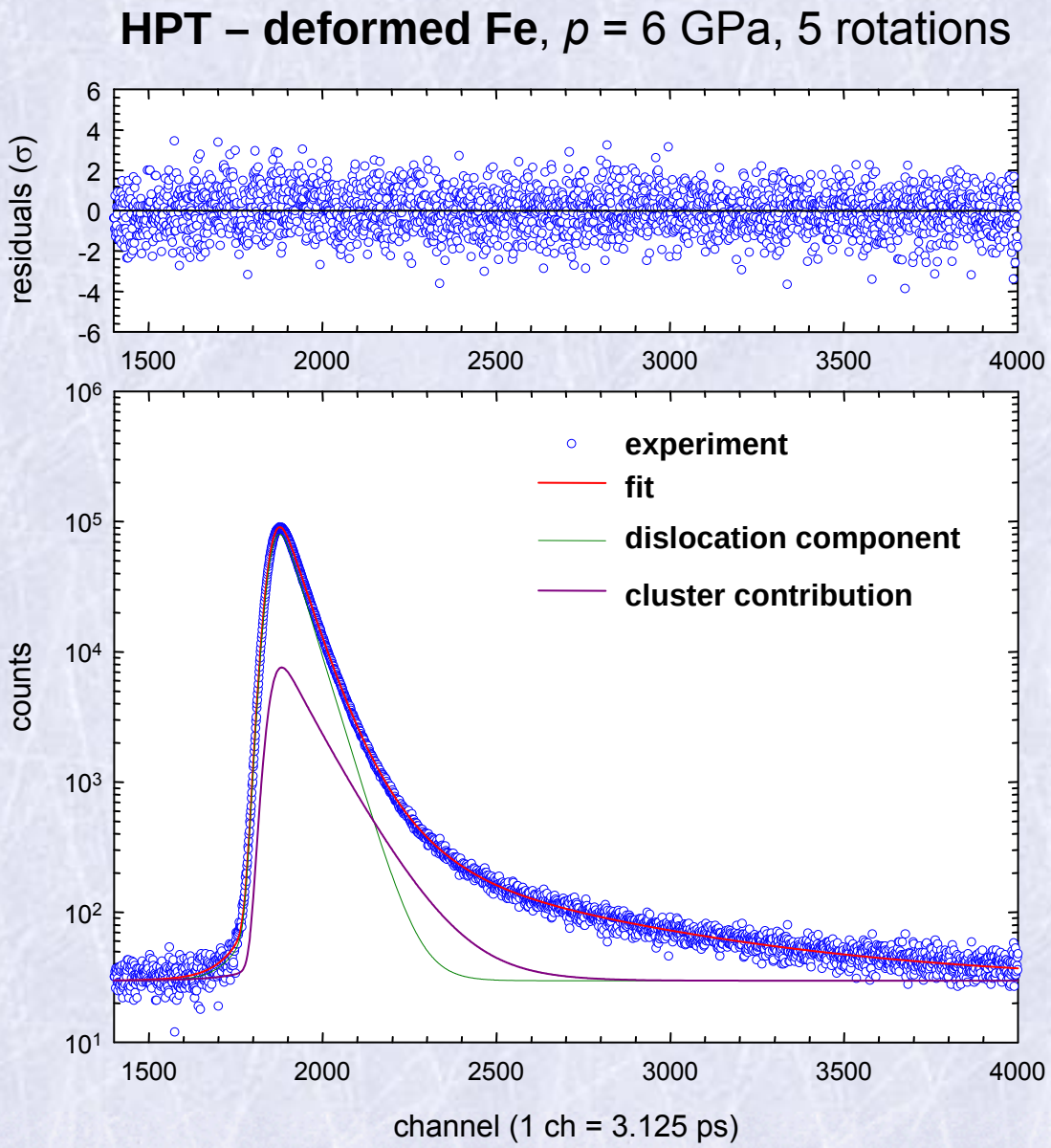

Decomposition of positron lifetime spectrum

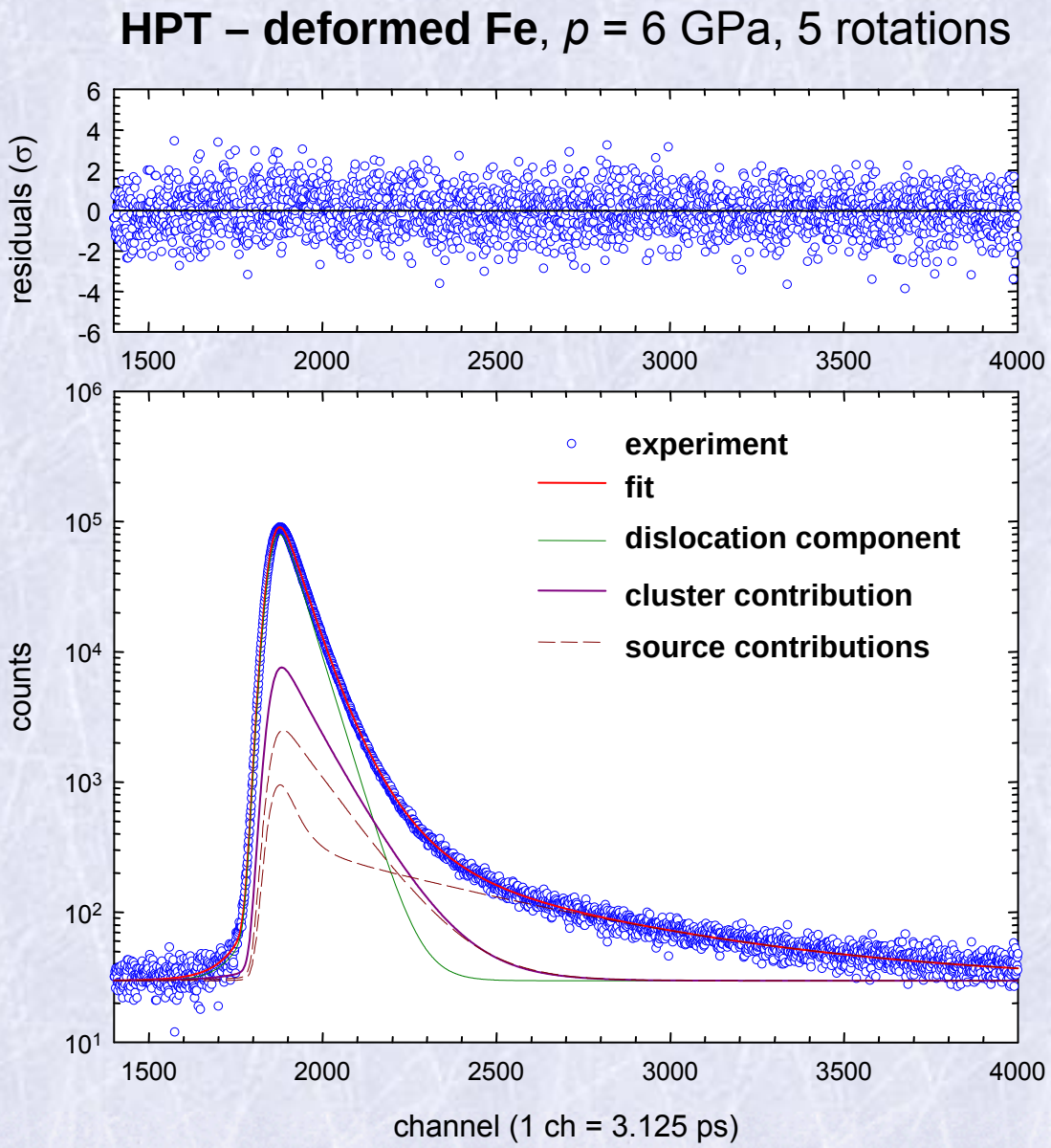

Decomposition of positron lifetime spectrum

- **goodness-of-fit: χ^2 test**
- χ^2 coefficient is improved compared to the traditional approach
- Poisson distribution of vacancy clusters is in good agreement with experiment

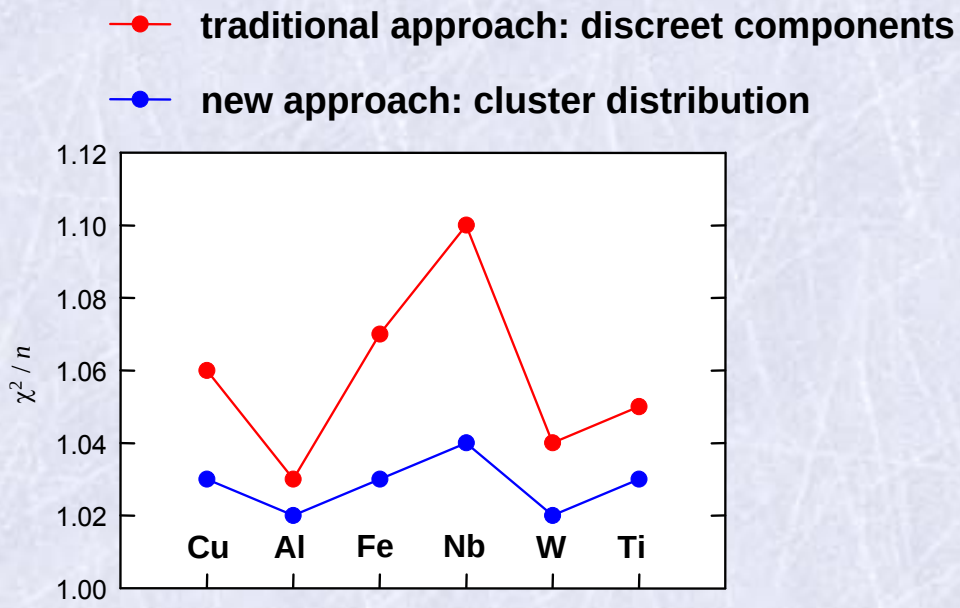

Results: comparison of various HPT – deformed metals

- HPT-deformed metals, *p* = 6 GPa, 5 HPT revolutions
- measured in the centre of the sample disk

sample	τ_1 (ps)	I_1 (%)	τ_2 (ps)	I_2 (%)	ν_d	I_d (%)
Cu, fcc	-	-	164(1)	73.3(8)	3.7(2)	26.7(8)
Al, fcc	158(1)	86.5(4)	240(3)	10(1)	40(3)	3.5(4)
Fe, bcc	-	-	150.8(8)	89.8(2)	11.3(5)	10.2(3)
Nb, bcc	-	-	174(1)	91.2(3)	3.0(2)	8.8(5)
W, bcc	-	-	161.6(6)	90.5(5)	13(1)	9.5(7)
Ti, hcp	-	-	182(1)	96.3(5)	39(2)	3.7(7)

free positrons

dislocations

vacancy clusters
(size distribution)

Results: comparison of various HPT – deformed metals

- HPT-deformed metals, *p* = 6 GPa, 5 HPT revolutions
- measured in the centre of the sample disk

size distribution P(*N*) of vacancy clusters

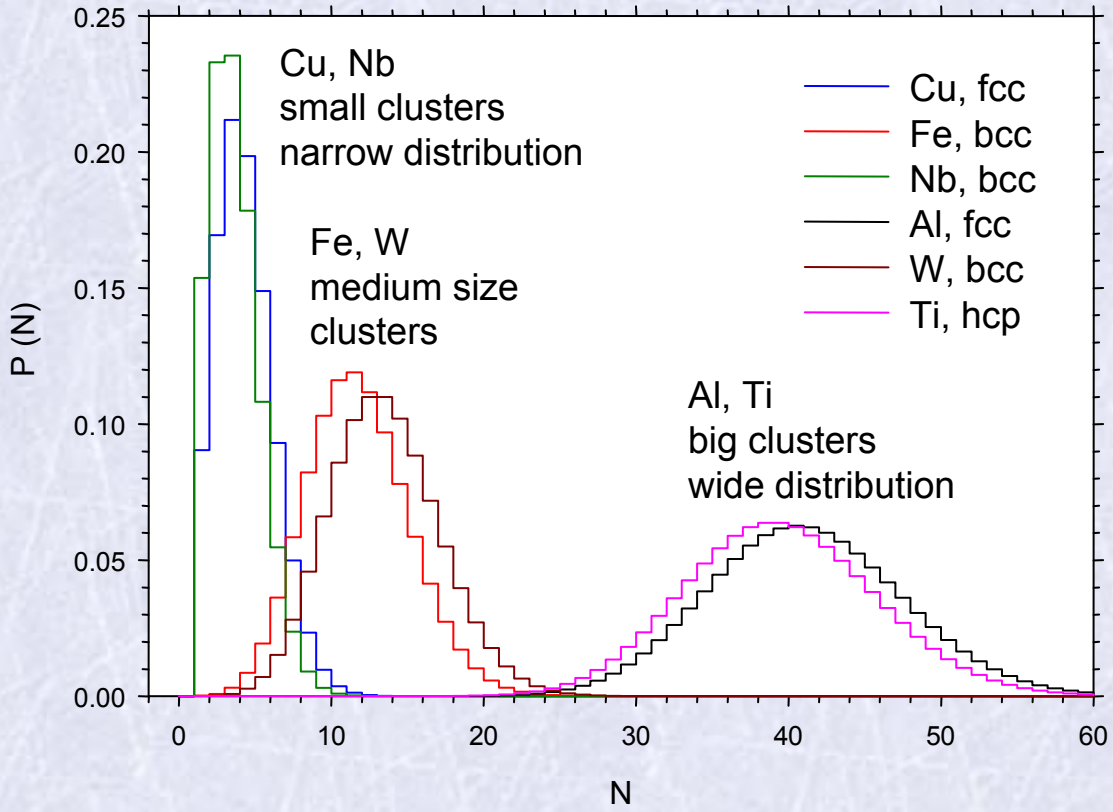

Results: comparison of various HPT – deformed metals

- HPT-deformed metals, *p* = 6 GPa, 5 HPT revolutions
- measured in the centre of the sample disk

size distribution P(*N*) of vacancy clusters

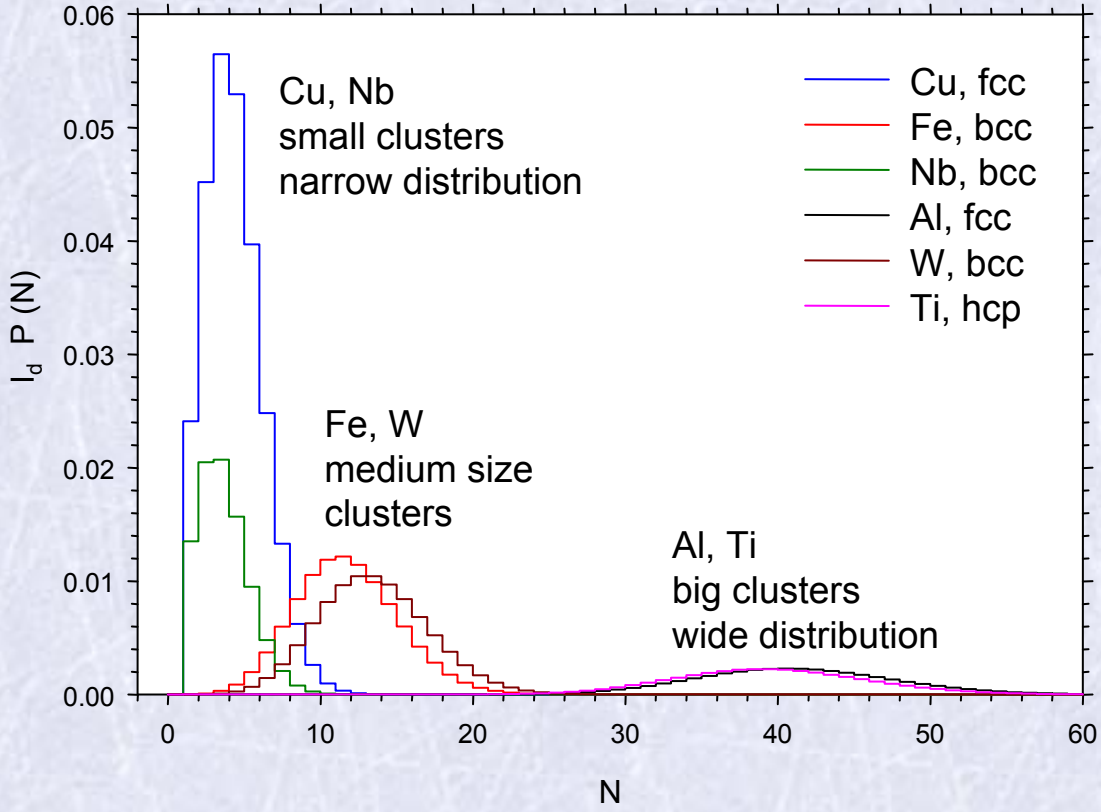

Results: comparison of various HPT – deformed metals

- HPT-deformed metals, *p* = 6 GPa, 5 HPT revolutions
- **No direct relation to metal structure**

size distribution P(*N*) of vacancy clusters

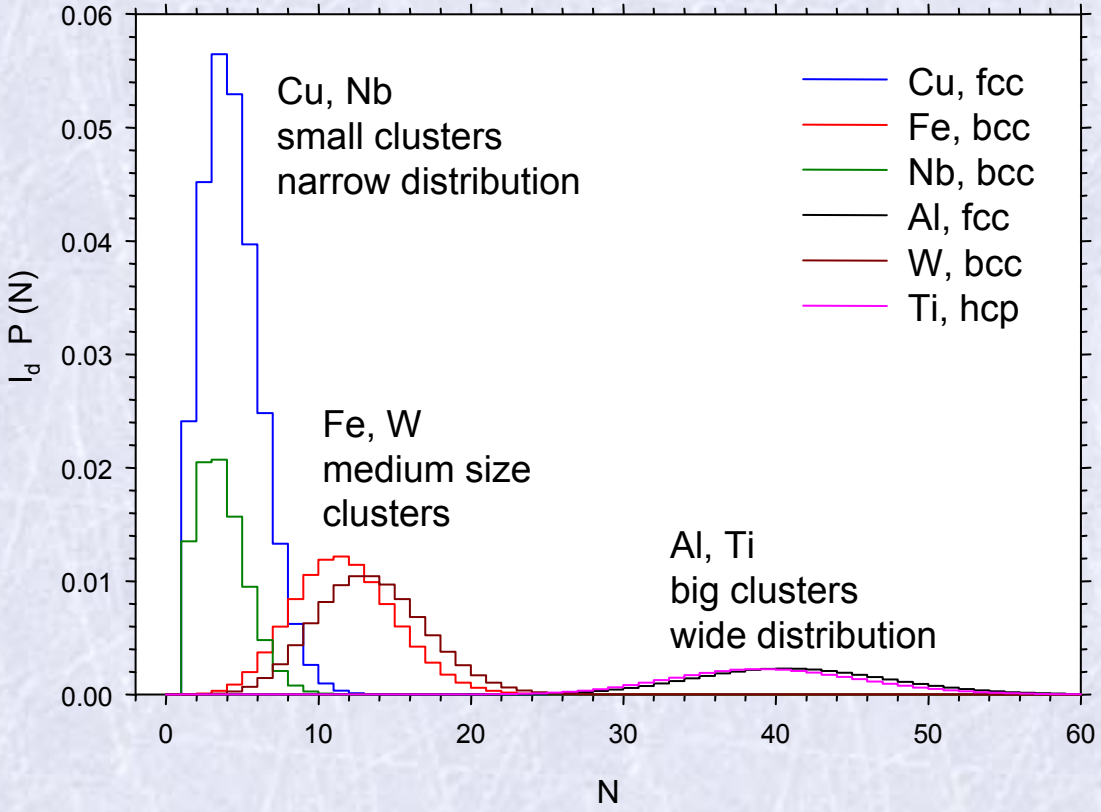

Results: comparison of various HPT – deformed metals

- HPT-deformed metals, p = 6 GPa, 5 HPT revolutions
- **No direct relation to vacancy formation energy $E_{v,f}$**

size distribution P(N) of vacancy clusters

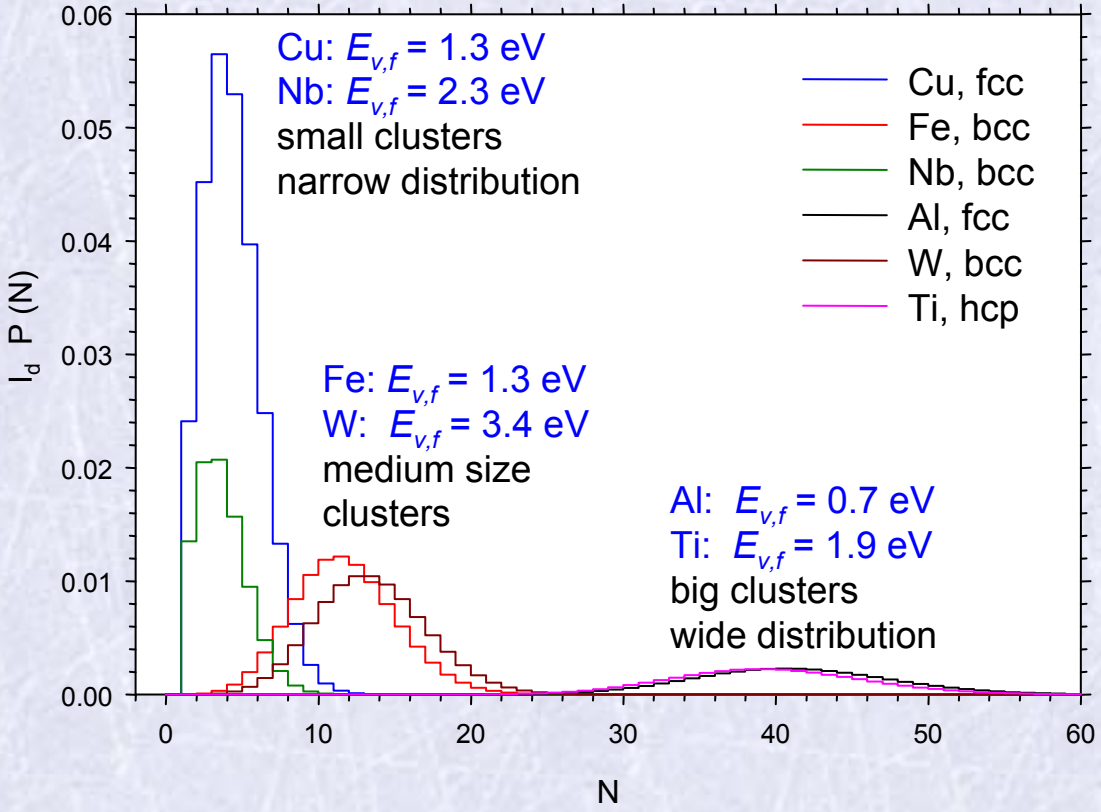

Results: comparison of various HPT – deformed metals

- HPT-deformed metals, p = 6 GPa, 5 HPT revolutions
- **low activation energy E_m for vacancy migration leads to big clusters**

size distribution P(N) of vacancy clusters

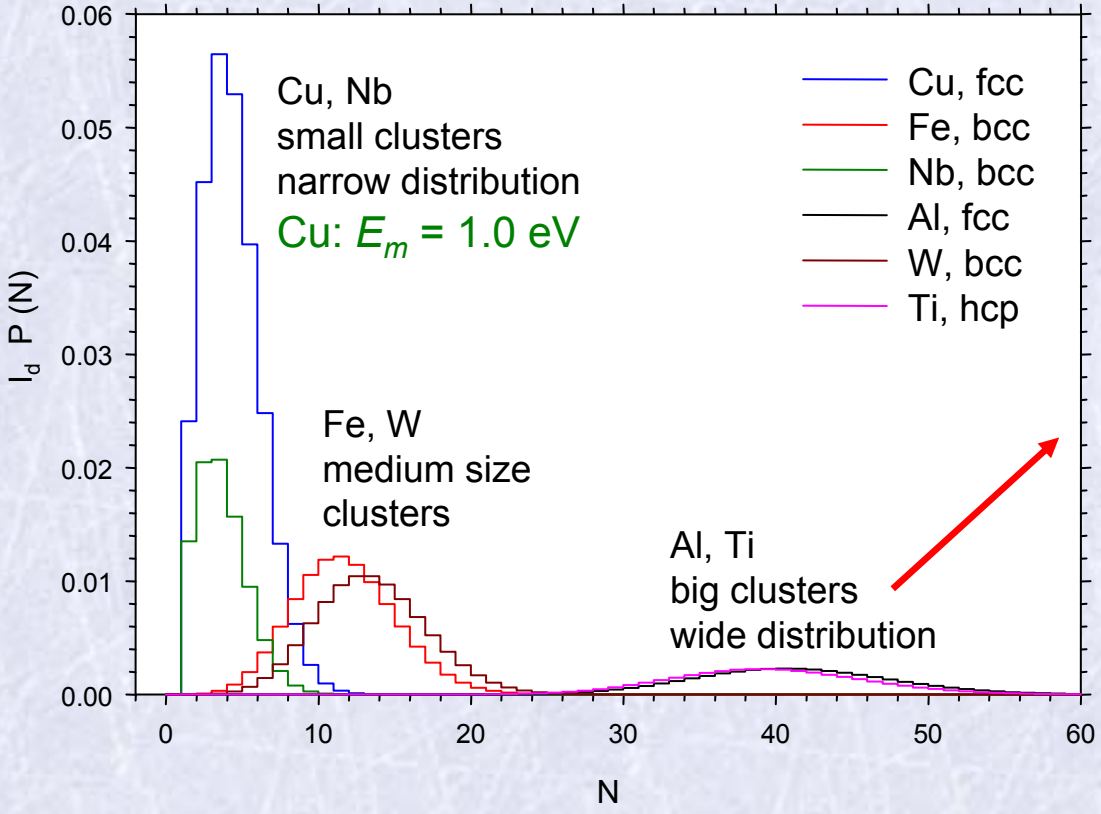

low activantion energy for migration of vacancies
Ti: E_m = 0.43 eV
Al: E_m = 0.42 eV

Production of deformation-induced vacancies

- production rate of deformation-induced vacancies

$$\Pi = \alpha \frac{\sigma \Omega_0}{E_f} \dot{\varepsilon}$$

strain rate

- coefficient $\alpha \approx 0.1$ G. Gottstein et al. *Acta Mater.* **23**, 641 (1975)
- σ : applied stress
- Ω_0 : atomic volume
- E_f : vacancy formation energy
- $\dot{\varepsilon}$: strain rate

HPT deformation

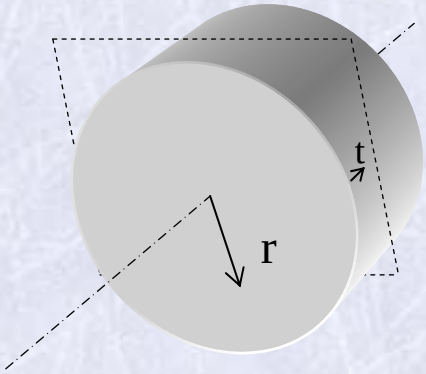

- strain rate increases with r

Development of deformation-induced vacancy clusters

- **HPT-deformed Cu, *p* = 6 GPa**
- comparison of centre and periphery of the sample disk
- production rate of vacancies is higher at the periphery

↓

- **higher vacancy concentration**
- **bigger vacancy clusters**

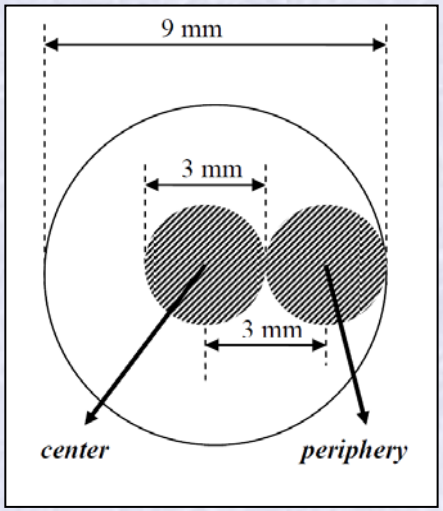

1 HPT revolution

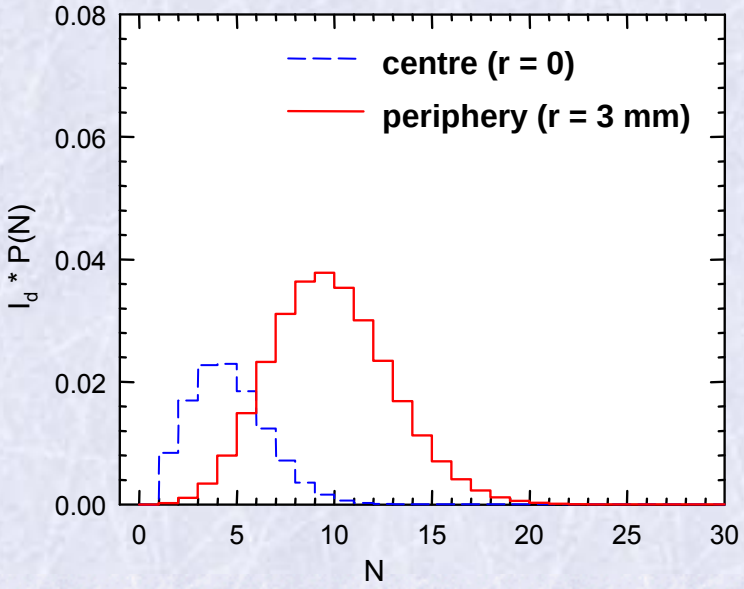

25 HPT revolutions

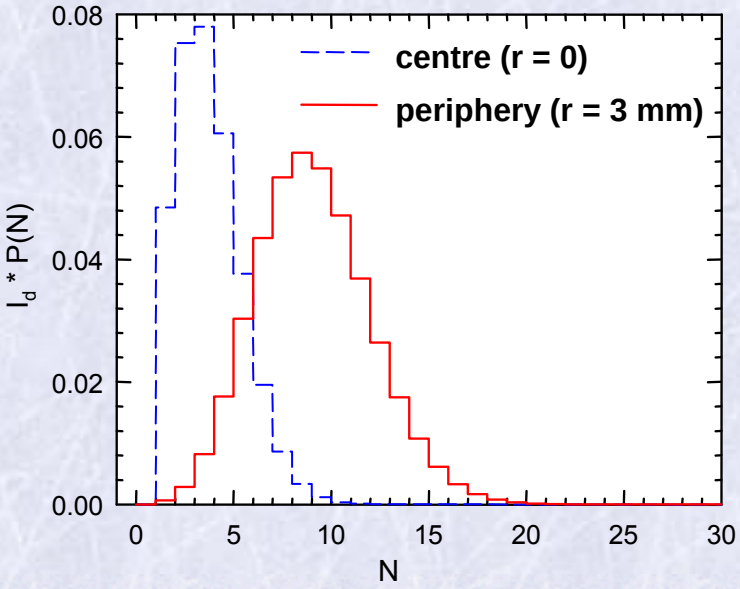

Development of deformation-induced vacancy clusters

- **HPT-deformed Cu, *p* = 6 GPa**
- comparison of centre and periphery of the sample disk
- periphery: higher vacancy concentration, bigger clusters
- increasing number of HPT revolutions:
  - **concentration of vacancies increases**
  - **size distribution remains constant**

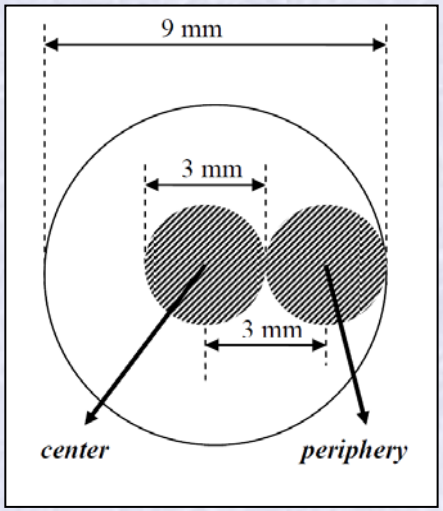

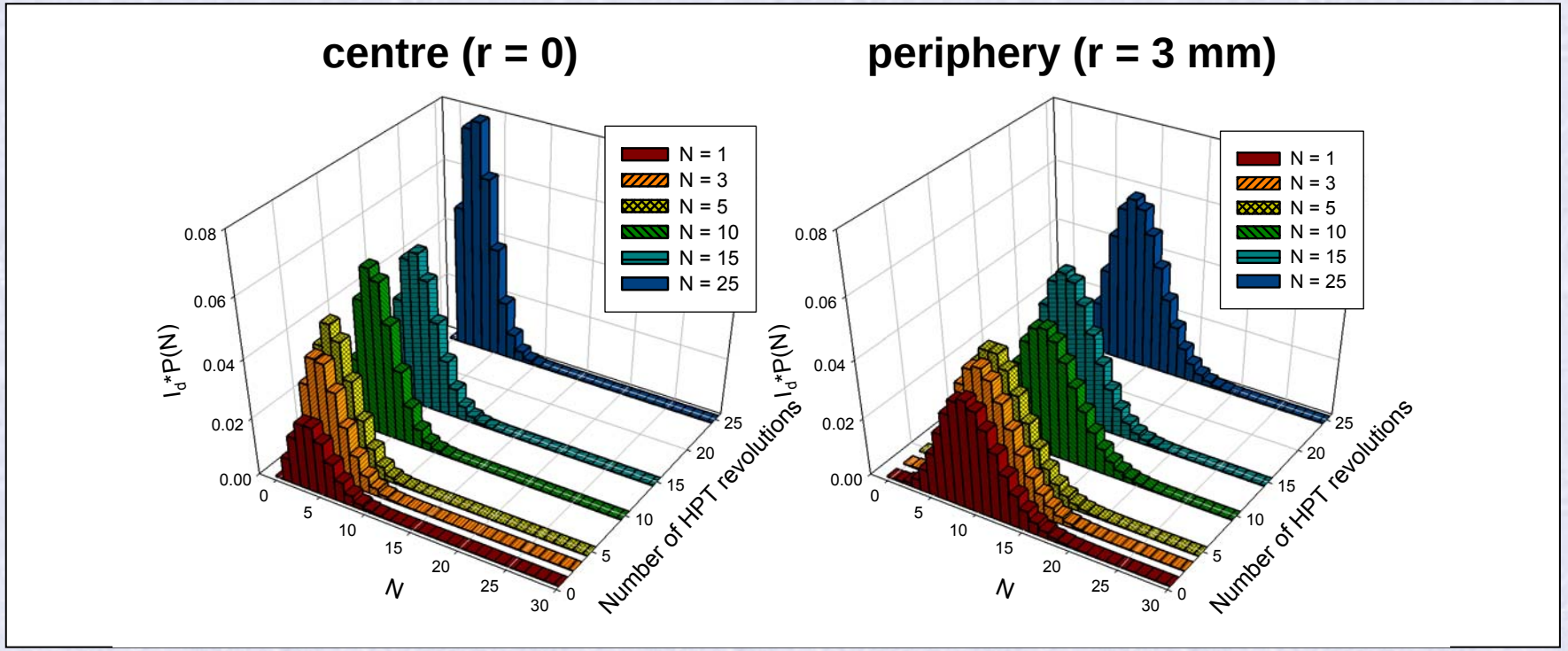

Mapping of structural homogeneity - microhardness (HV)

UFG Cu, HPT deformed, p = 6 GPa

• HV is sensitive to dislocation density and grain size but not to vacancies

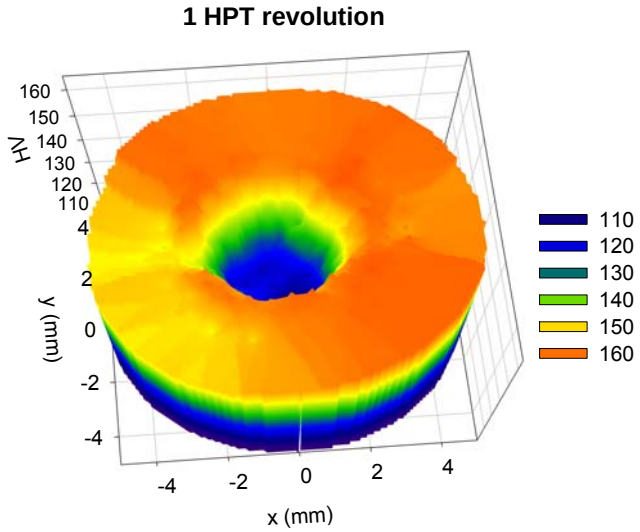

$$e = \ln\left(\vartheta r / l\right)$$

- e - true log. strain
- ϑ - rotation angle
- r - distance from center
- l - sample thickness

Mapping of structural homogeneity - microhardness (HV)

UFG Cu, HPT deformed, p = 6 GPa

- HV is sensitive to dislocation density and grain size but not to vacancies

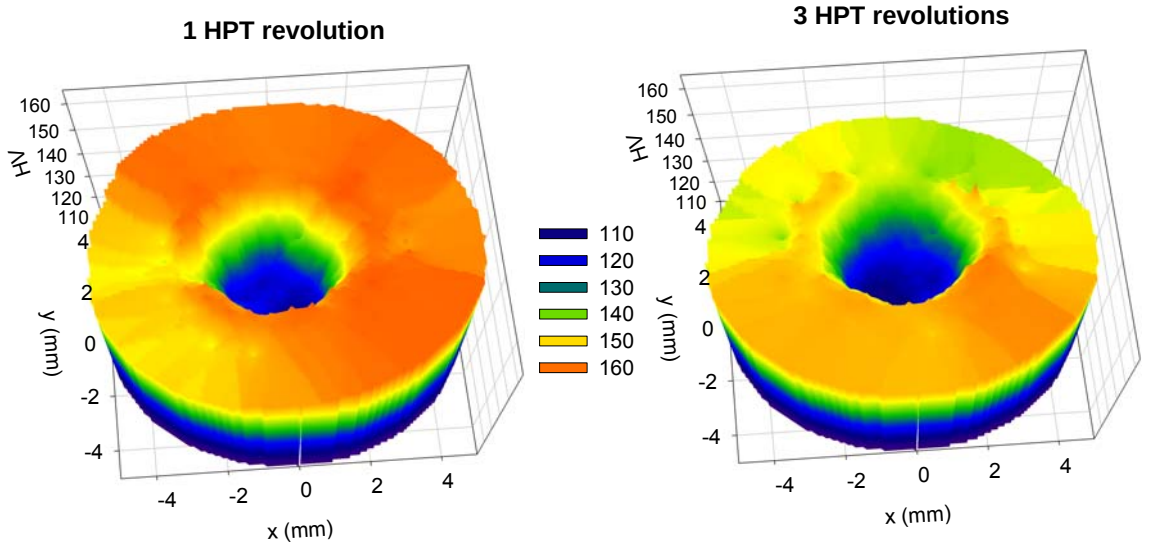

$$e = \ln\left(\vartheta r / l\right)$$

- e - true log. strain
- ϑ - rotation angle
- r - distance from center
- l - sample thickness

Mapping of structural homogeneity - microhardness (HV)

UFG Cu, HPT deformed, p = 6 GPa

- HV is sensitive to dislocation density and grain size but not to vacancies

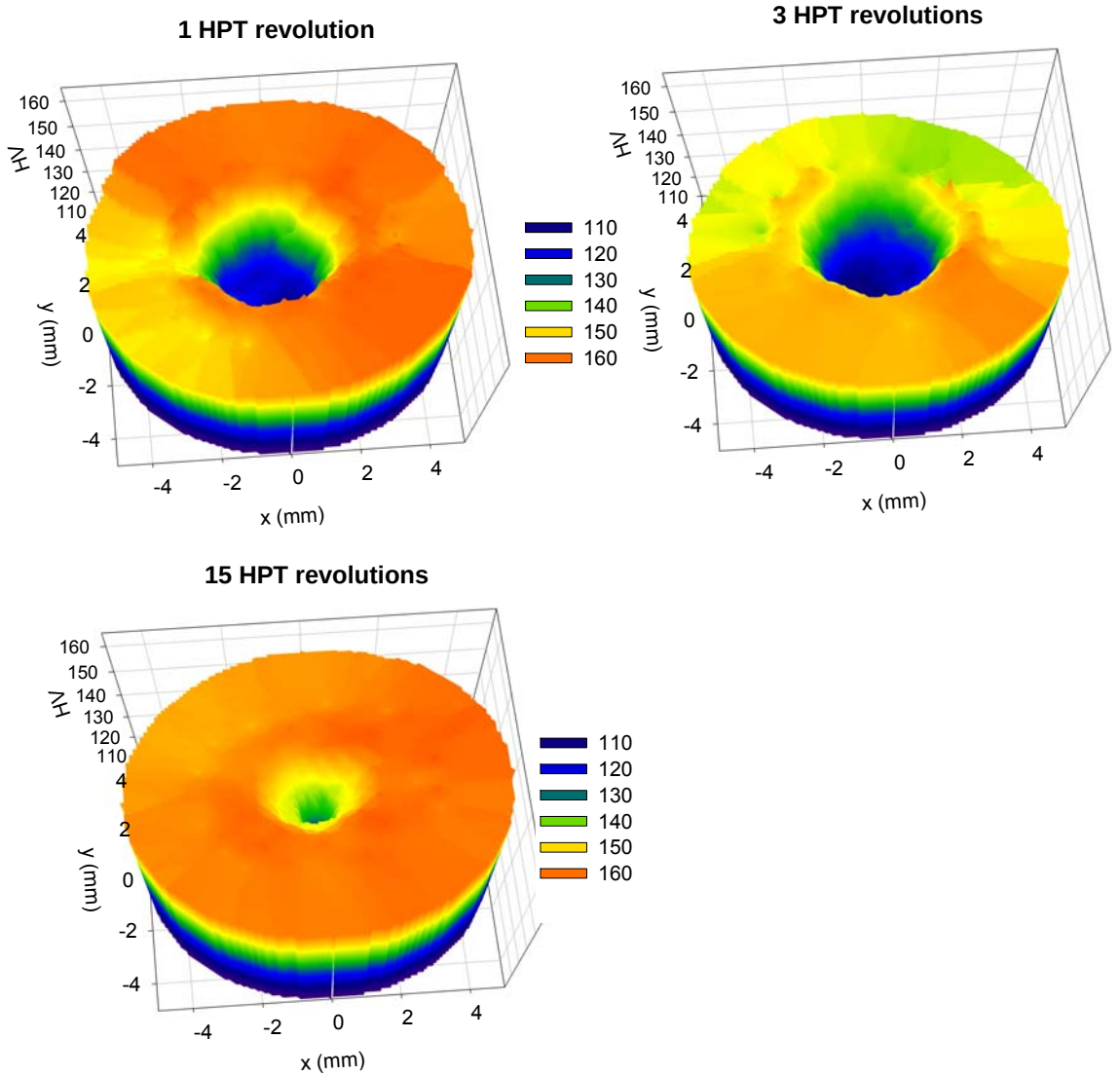

$$e = \ln\left(\vartheta r / l\right)$$

- e - true log. strain
- ϑ - rotation angle
- r - distance from center
- l - sample thickness

Mapping of structural homogeneity - microhardness (HV)

UFG Cu, HPT deformed, p = 6 GPa

- HV is sensitive to dislocation density and grain size but not to vacancies

↓

- homogeneous HV after 25 HPT revolutions

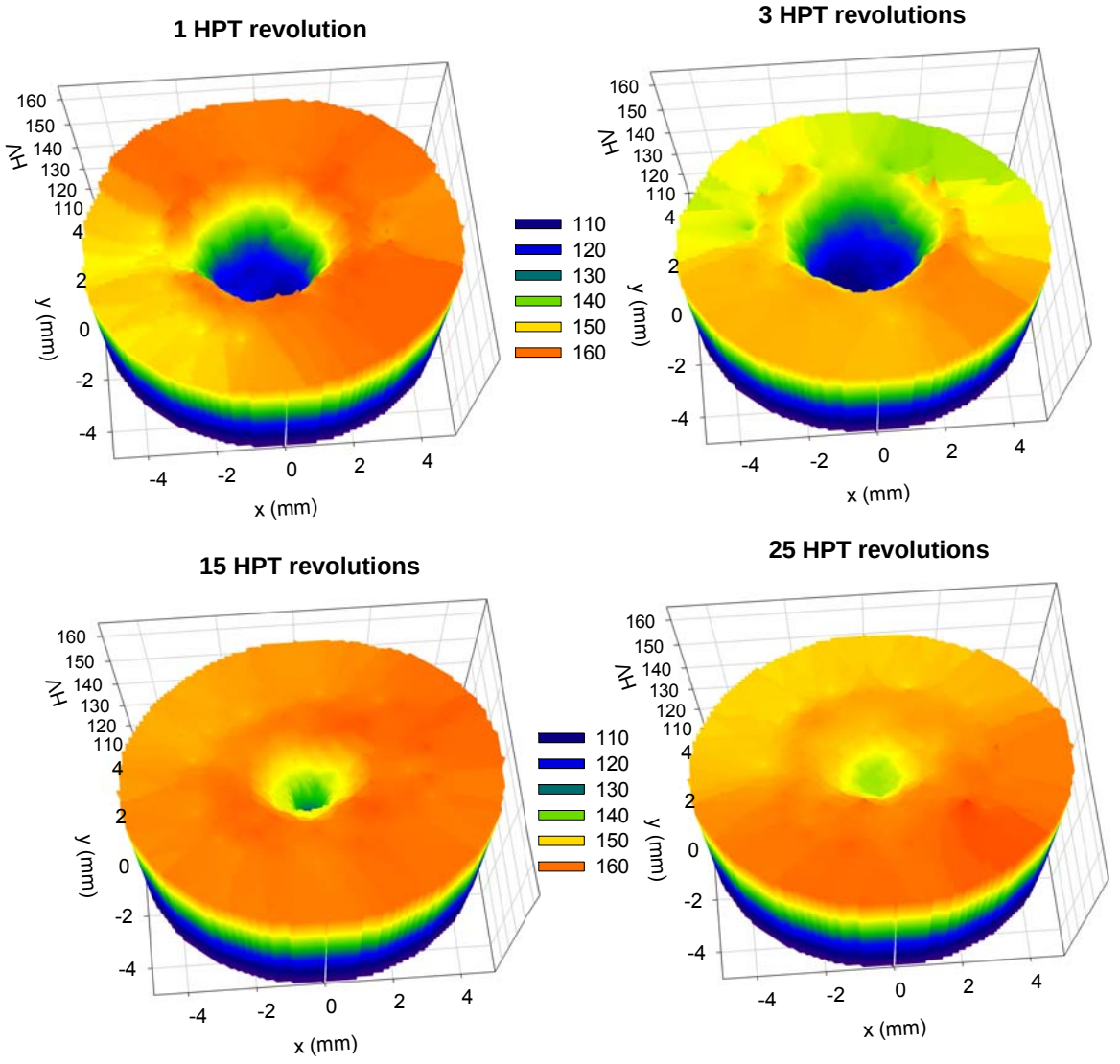

$$e = \ln(\vartheta r / l)$$

- e - true log. strain
- ϑ - rotation angle
- r - distance from center
- l - sample thickness

Mapping of structural homogeneity - *S* parameter

UFG Cu, HPT deformed, p = 6 GPa

- *S* parameter increases with r

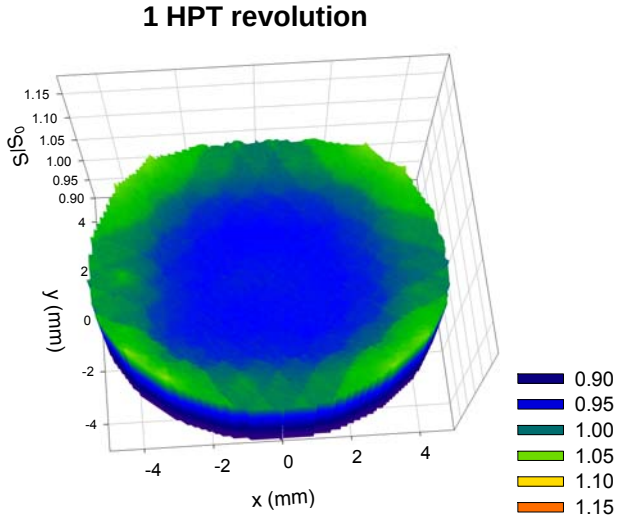

$$e = \ln\left(\vartheta r / l\right)$$

- e - true log. strain
- ϑ - rotation angle
- r - distance from center
- l - sample thickness

Mapping of structural homogeneity - *S* parameter

UFG Cu, HPT deformed, p = 6 GPa

- *S* parameter increases with r

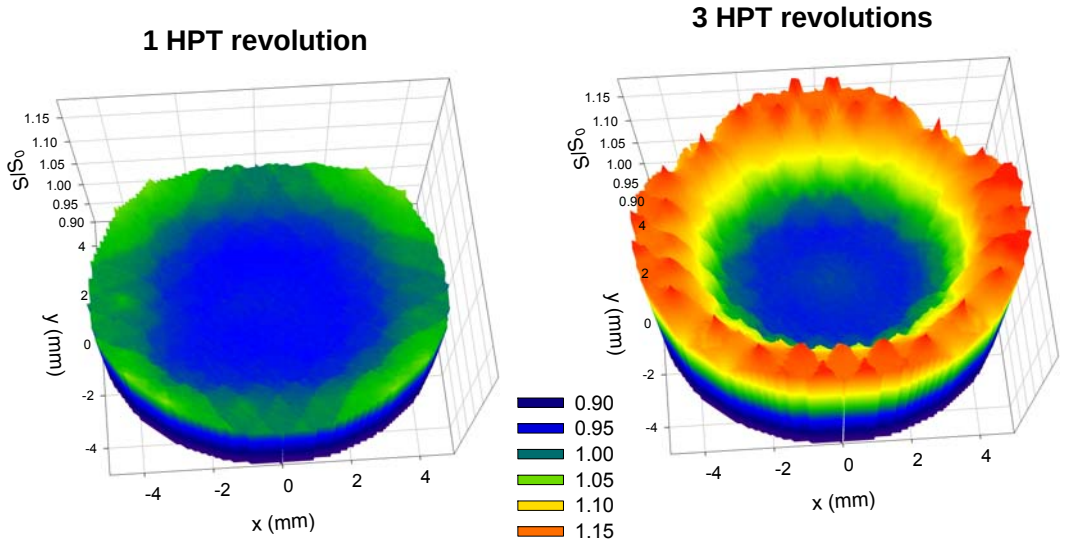

$$e = \ln\left(\vartheta r / l\right)$$

- e - true log. strain
- ϑ - rotation angle
- r - distance from center
- l - sample thickness

Mapping of structural homogeneity - *S* parameter

UFG Cu, HPT deformed, p = 6 GPa

- *S* parameter increases with r

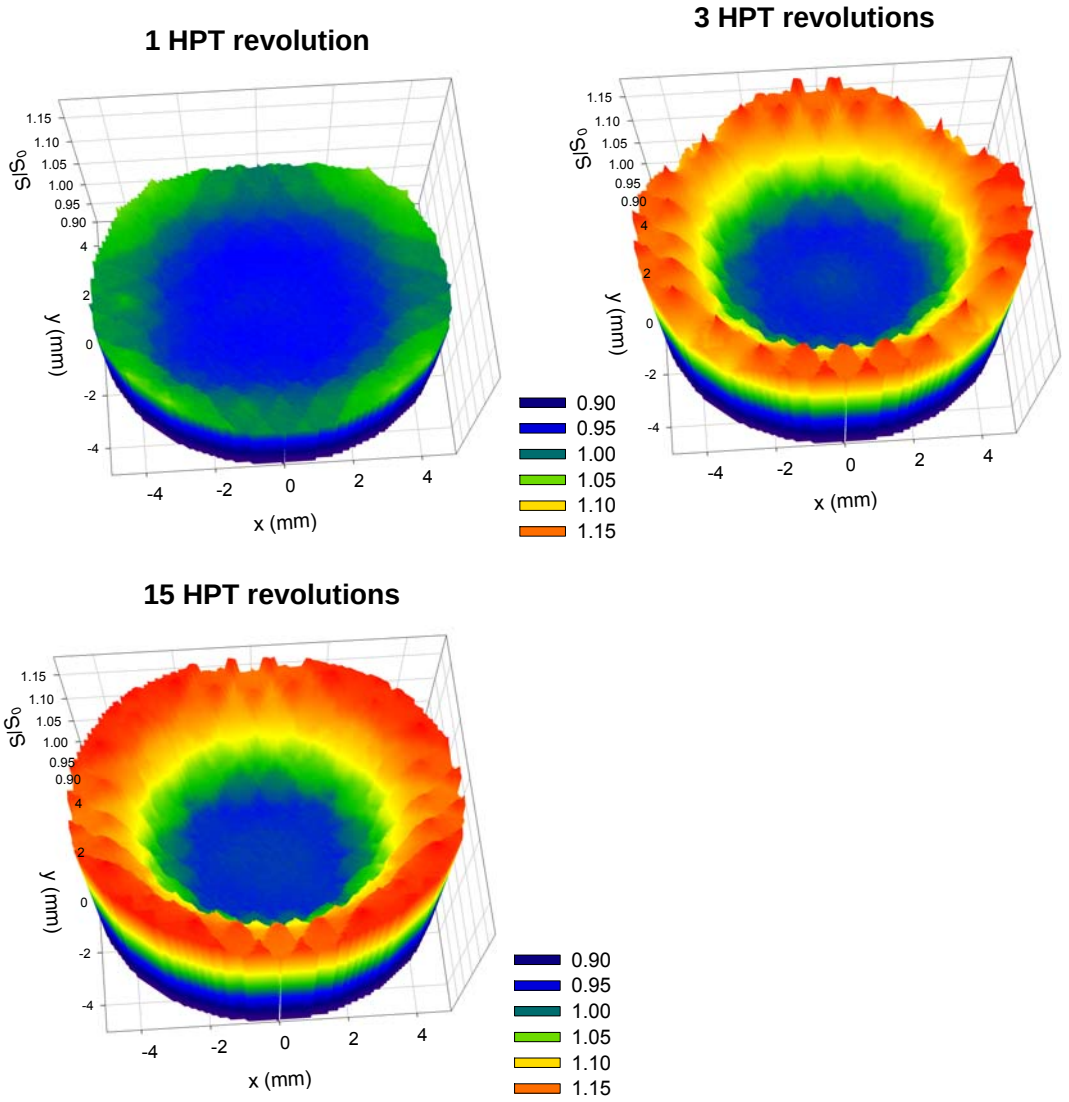

$$e = \ln(\vartheta r / l)$$

- e - true log. strain
- ϑ - rotation angle
- r - distance from center
- l - sample thickness

Mapping of structural homogeneity - *S* parameter

UFG Cu, HPT deformed, p = 6 GPa

- *S* parameter increases with r
- increasing size of vacancy clusters
- spatial distribution of vacancies is from being uniform even after 25 rotations

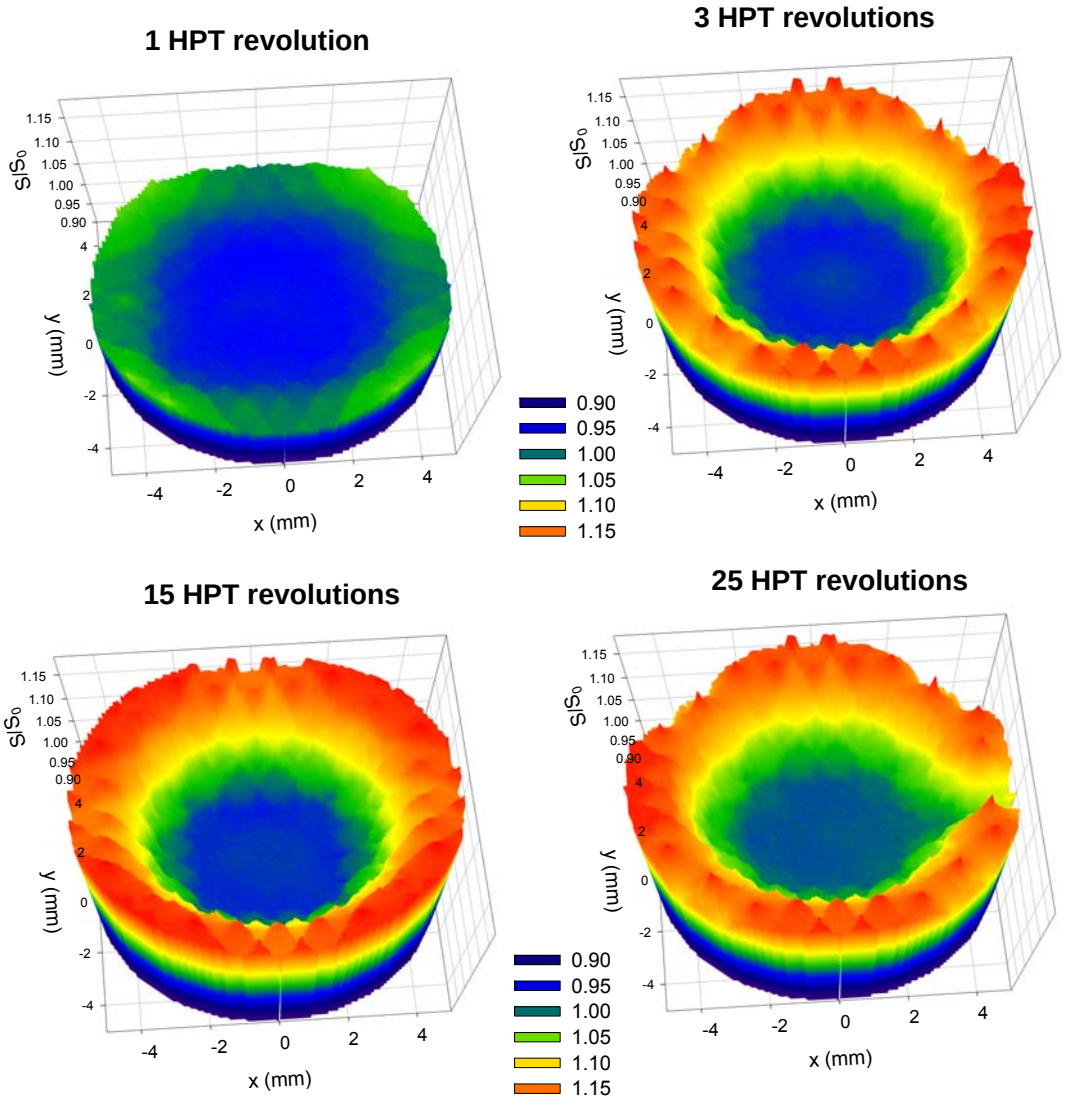

$$e = \ln(\vartheta r / l)$$

- e - true log. strain
- ϑ - rotation angle
- r - distance from center
- l - sample thickness

Mapping of structural homogeneity - comparison of HV and *S* parameter

UFG Cu, HPT deformed, p = 6 GPa, 25 HPT revolutions

- **microhardness (HV)** is influenced by
  - grain size
  - dislocation density

after 25 HPT revolutions HV becomes uniform

- **S parameter** is influenced by
  - dislocation density
  - cocentration and size of vacancy clusters

after 25 HPT revolutions S is higher at the periphey

- **spatial distribution of vacancies is from being uniform even after 25 rotations**

microhardness

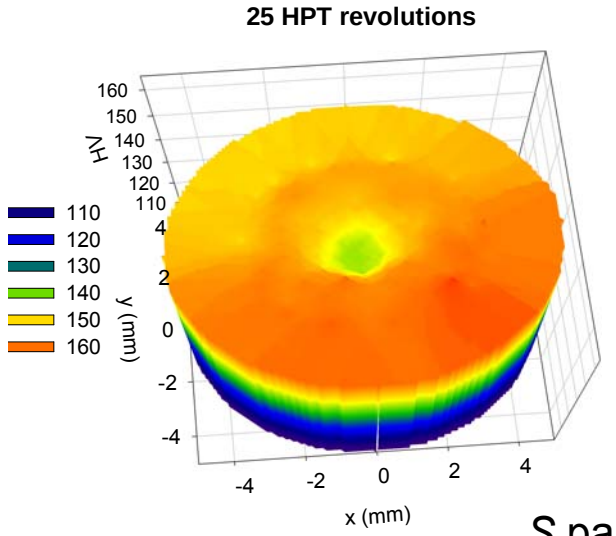

S parameter

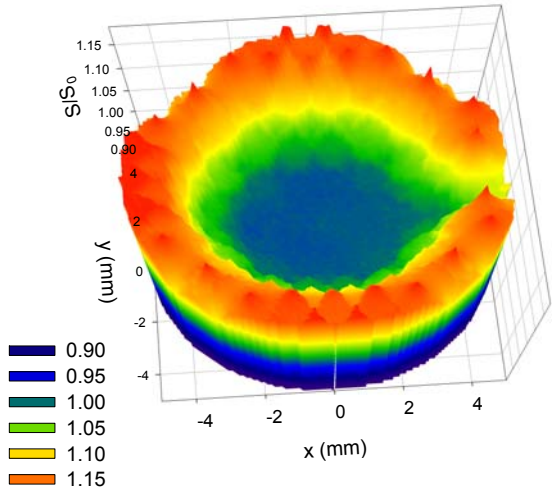

Conclusions

- Severe plastic deformation introduces vacancies which subsequently agglomerate and form vacancy clusters
- Size distribution of vacancy clusters was determined by positron lifetime spectroscopy combined with *ab-initio* theoretical calculations
- Poisson distribution of vacancy clusters is in good agreement with experiment
- Size distribution of vacancy clusters in various metals is considerably different
- Size of vacancy clusters increases with the strain rate due to higher production rate of vacancies
- As a consequence in HPT-deformed samples the size of vacancy clusters increases with the radial distance from the centre

Acknowledgements

- The authors are grateful to Jan Kuriplach for providing them with ATSUP code for *ab-initio* theoretical calculations
- This work was supported by The Czech Science Foundation (project P108/12/G043)